When to Lock, Not Whom: Managing Epidemics Using Time-Based Restrictions*

Yinon Bar-On, Weizmann Institute of Science, Israel
Tanya Baron, Ben Gurion University, Israel
Ofer Cornfeld, BFI, Israel

Eran Yashiv, Tel Aviv University, Israel; CfM (LSE), UK; and CEPR†

December 9, 2022

Abstract

We present novel policy tools to manage epidemics. Rather than using prevalent population restrictions, these policy strategies are based on cyclical time restrictions. Key findings on the outcomes of such policy strategies include: a significant improvement of social welfare, substantially lessening the trade-offs between economic activity and health outcomes; optimally-derived timings of interventions are shown to suppress the disease, while maintaining reasonable economic activity; and outcomes are superior to the actual experience of New York State and Florida over the course of 2020.

Key words: epidemic/pandemic management, cyclical strategies, social planner, endogenous individual response, lockdown, time restrictions, positive analysis, policy frontier.

JEL codes: E23, E61,E65, I12, I18.

We thank Philipp Kircher, Marc Lipsitch, and especially Gadi Barlevy and Ben Moll for useful exchanges, two anonymous referees and the RED editor, David Lagakos, for very helpful comments, seminar participants at UCL, LSE, Aix-Marseille, the Center for Combatting Pandemics at TAU, Haifa, IEA meetings, and Tel Aviv for comments, and Roy Cnaan for research assistance. Any errors are our own.

†*Corresponding author.* yashiv@tauex.tau.ac.il; https://www.yashiv.sites.tau.ac.il/

When to Lock, Not Whom: Managing Epidemics Using Time-Based Restrictions

1 Introduction

The COVID19 pandemic has created a global health and economic crisis of a magnitude not experienced since the Great Influenza Pandemic of 1918-1919. After 33 months, about 630 million people have become infected, about 6.6 million people worldwide have died, and estimates of excess deaths are more than three times as high;[1]IMF (2022) reported a 3.1% drop in world GDP in 2020, and a 4.5% drop in the advanced economies. The death toll in the U.S. is almost 1.1 million; the declines in U.S. GDP and consumer expenditures for 2020 have been -3.4% and -3.8%, respectively.

We address the issue of policy responses to the pandemic, providing an analysis of new time-based tools to manage epidemics. These policy strategies were proposed in epidemiologically-grounded work by Karin et al (2020). The contribution of our paper is the economic analysis of these new policy tools. The proposed policy consists of alternating periods of work and lockdown, at pre-defined frequencies, for the entire population. We present both normative and positive analyses. The former applies to future pandemics or epidemics while the latter evaluates policy against real world benchmarks in the U.S. using data.

The proposed policy tools are particularly relevant in light of the difficulties experienced by policymakers in finding a policy strategy that lessens the tradeoffs involved. In theory, targeted population lockdowns could constitute "fine tuning" of lockdown measures, which would serve to lessen any economic cost. In practice, however, it turned out to be challenging to identify sub populations to be allowed unrestricted economic activity, while imposing restrictions on other population groups. Political and moral issues, as well as practical implementation issues, have come into play. The time-based public health management policy avoids these difficulties, taking time, rather than population, as the medium of restrictions.

Our model lies within a line of COVID19 research in Economics, which posits a planner problem. The planner formulates an optimal policy of Non-Pharmaceutical Interventions (NPIs), and in particular, lockdowns, subject to a model of disease dynamics, taking into account vaccine arrival. The planner trades off the costs of public health outcomes, such as breach of ICU capacity and death, with the economic costs of suppression policy, including declines in production. Prominent contributions in this line of literature include Acemoglu, Chernozhukov, Werning, and Whinston (2021), Alvarez, Argente, and Lippi (2021), Brotherhood, Kircher, Santos, and Tertilt (2021), Brotherhood and Jerbashian (2020), Farboodi, Jarosch, and Shimer (2021), and Jones, Philippon, and Venkateswaran (2021). Our analysis pertains to new policy strategies, which were not considered in the literature.

[1]See https://ourworldindata.org/covid-deaths

We highlight five dimensions related to time:

(i) From the normative perspective, we analyze policy that relies on *time restrictions*. Such policy is an alternative to policy based on restrictions of sectors, age groups, regions, or other targeted population groups. The success of the policy hinges on two mechanisms that operate over time. In lockdown days, the disease is suppressed through exogenous government-imposed restrictions. In work days, the disease is suppressed through the endogenous rational behavior of the population. This combination allows the effective reproduction number to be kept at around 1 on average. Notably, a full, prolonged lockdown is not needed to keep death rates low. All that is needed is to have the open periods short enough, backed up by rational precaution of the population, and followed by lockdown periods of reasonable length ahead of the next re-opening.

(ii) The epidemiological rationale for the proposed policy is, inter alia but not exclusively, based on the *timescales of virus transmission*. The idea is that for every 14 day period, there will be k days of work and $14 - k$ days of lockdown. This number, k, uses the timescales of the virus against itself, taking into account a latent period after exposure, whereby the infected person does not infect others. In other words, the epidemiological cost of open days is mitigated by the fact that individuals do not become infectious immediately. The epidemiological benefit of lockdown days is enhanced because the schedule locks down the economy when individuals are at their most infectious.

(iii) Using an optimizing social planner model, the control variables for this policy are *the timing of the various measures* – initial lockdown, the cyclical policy phase, and release. Hatchett, Mecher, and Lipsitch (2007) highlight the idea that imposing NPIs early in an epidemic can significantly reduce mortality. In the current paper, the exploration of timing issues, both start time and duration, are at the heart of the analysis.

(iv) This policy is compared to a prevalent policy path which sets lockdown and release as *functions of disease prevalence, which is time-varying*. Specifically, the latter uses trigger thresholds, such as the number of persons hospitalized in ICU in a given period of time, and gives rise to the pattern of recurrent lockdown and release observed in the U.S. and other countries since the start of COVID19.

(v) The proposed policy is subsequently compared to the actual experience of New York State (NYS) and Florida. The outcomes observed for NYS turn out to depend crucially on *the timing of the policies undertaken;* those for Florida reveal particular policy preferences.

We explicitly model the dynamic path for the reproduction parameter, reflecting both rational individual behavior and the effects of lockdown policy. Thus, we model the endogenous response by individuals, who adjust to the new environment and behave accordingly. Additionally, government interventions in the form of lockdowns induce behavioral change. These elements are included in a model whereby individuals maximize utility and a social planner maximizes a welfare function, which incorporates individual utility. We then take the model to the data and use the resulting estimates to calibrate the relevant parameters, which we subsequently use in simulations.

The social planner in our model uses a PDF in order to form ex-ante expectations of vaccine arrival time. This serves three key roles; first, it sets the horizon for the problem, acting as a rate of leaving the state of the pandemic. Second, it is an expression of the risk and uncertainty embodied in the planner problem. Third, relative to the interest rate, it plays the major quantitative role in discounting future streams. In our simulations vaccine arrival is realized after 540 days. Using these elements, our analysis quantifies outcomes in terms of social welfare. We simulate the optimal cyclical policies and examine their health and economic implications.

The cyclical policy is compared to four non-cyclical benchmarks: two polar cases, of no policy intervention (i.e., no lockdown) or full lockdown till vaccine arrival; a single time span lockdown policy, whereby the starting date and the duration are chosen optimally; and a theoretical path trying to mimic a real-world rationale, whereby the planner chooses thresholds for multiple lockdowns in terms of the critically ill. Subsequently, and additionally, we evaluate the time-based policy tools in relation to the actual experience of NYS and Florida in 2020.

We plot the policy plans in terms of a policy possibilities frontier. These show the outcomes of optimal planner policies, using a two-dimensional graph of the death toll per 1 million people and the value of lost output, in annual GDP terms. Movement along the frontier occurs as the policy instrument in use changes, or as the weight assigned to fatalities in the planner objective function changes, or as the lethality of the disease changes.

Our analysis yields the following key findings.

First, the policy instruments, based on time restrictions, provide for significant improvement, substantially lessening the trade-offs involved relative to the four non-cyclical benchmarks. The latter are situated in points on the graph beyond the frontier.

Second, we quantify social welfare costs. These are given in utility terms and in Present Discounted Value (PDV) consumption terms. Using the consumption loss measure, comparing actual consumption to the pre-COVID steady state (formally defined below), the different cyclical strategies place these losses at 22% to 26% , the no intervention policy results in 36%, full lockdown in 29%, optimal lockdown duration in 27%, and the thresholds strategy in 25%. The underlying rationale for the improvement is that cyclical strategies allow the planner to achieve similar death tolls with fewer lockdowns, or to reduce the death toll dramatically without a significant damage to output. These results are due to the optimally-derived timings of intervention (for example, "front loading" interventions is beneficial in specific cases, which are spelled out) and the ability of the cyclical strategies to suppress the disease while maintaining a reasonable level of economic activity.

Third, using daily data from March 2020 to early 2021, optimal cyclical policies fare much better than actual experience in the states of New York and Florida. When deriving this result, we use estimated state-specific parameters in the simulations.

Importantly, the benefits of the time-based policy tools that we find are

likely to be a lower bound of their true advantage over policy strategies that have been implemented. This is so because, for tractability, we are not giving the planner full flexibility when applying the cyclical tools. Similarly, we do not quantify additional benefits, such as predictability of production, gains in non-COVID health matters, transparency, ease of communication, and fairness.

We note that the idea of a cyclical strategy, which is at the focal point of the normative analysis of our analysis, has been brought to the attention of policymakers (see Yashiv (2020), Alon and Yashiv (2020), and Alon, Milo and Yashiv (2020)) and has been considered or implemented by a host of firms and educational institutions in the U.S., in Europe, and in Latin America. Online Appendix A provides elaboration.

The paper proceeds as follows: Section 2 discusses the model, including the policies we propose, on which we further elaborate in online Appendix A. Section 3 presents the calibration and the solution methodology. Section 4 presents the results. Section 5 explores the underlying mechanism. Section 6 examines the relation between the model planner solution and actual outcomes in two U.S. states – NYS and Florida. Section 7 concludes. Online Appendices B and C provide further elaboration.

2 The Model

We model an optimizing social planner who operates within a SEIR model of the epidemic and a model of the macroeconomy with optimizing agents responding to the epidemic. We elaborate on the novel policy strategies based on time restrictions.

2.1 The Evolution of the Epidemic

We analyze the evolution of the epidemic in two complementary blocks – infection transmission and clinical progression.

2.1.1 The Infection Transmission Block

The infection transmission block is characterized by the SEIR-Erlang model, reflecting the epidemiological properties of COVID19. The model is essentially based on the seminal contribution of Kermack and McKendrick (1927). Its present form is discussed in Champredon, Dushoff, and Earn (2018). See Bar-On, Baron, Cornfeld, Milo and Yashiv (2021) for a more detailed analysis, where we explain the need for the two complementary model blocks. Before contacting the disease for the first time, a person is Susceptible (S). Once a person gets infected, disease progression is split into distinct compartments – Exposed (E), Infectious (I), and Resolved (R). We denote by β_t the infections transmission rate, σ, the transition rate from E to I, and γ, the transition rate from I to R. An infected individual spends some time in each compartment before moving on to the next one. The person is infectious only when in the I compartment, but not when residing in the preceding E compartment. The time durations

spent in the E and I compartments are known as the latent and infectious periods, respectively. Once people move to the Resolved stage, they no longer participate in disease transmission. With Poisson transition rates between compartments, the residence times in each of them are distributed exponentially, and thus have zero mode. Exponential distributions capture the mean but not the mode of the biologically accurate distributions of residence times, because in reality what most people spend in each stage is close to the mean of the distribution, rather than zero. Therefore, we split the E and I compartments into two sub-compartments and double the rate of transition. Now, the latent and infectious periods are the sum of the time spent in the E_1 and E_2 or I_1 and I_2 sub-compartments, respectively. Their distribution is the sum of exponentially distributed random variables, a special case of the Gamma distribution, known as the Erlang distribution. The means of Erlang distributions remain $1/\sigma$ and $1/\gamma$, but the modes are now near the means, as they should be. In the remainder of the paper we shall refer to this model as the $SEIR$ model, without noting the number of sub-compartments.

Graphically, this block is presented in panel a of Figure 1.

Figure 1

The following equations describe this block. Throughout, all stock variables are expressed as a fraction of the population.

$$\dot{S}_t = -\beta_t(I_{1t} + I_{2t})S_t \tag{1}$$
$$\dot{E}_{1t} = \beta_t(I_{1t} + I_{2t})S_t - 2\sigma E_{1t} \tag{2}$$
$$\dot{E}_{2t} = 2\sigma E_{1t} - 2\sigma E_{2t} \tag{3}$$
$$\dot{I}_{1t} = 2\sigma E_{2t} - 2\gamma I_{1t} \tag{4}$$
$$\dot{I}_{2t} = 2\gamma I_{1t} - 2\gamma I_{2t} \tag{5}$$
$$\dot{R}_t = 2\gamma I_{2t} \tag{6}$$

An important parameter is the reproduction number $\mathcal{R}_t$, which is the average number of people infected by a person, and is given by:

$$\mathcal{R}_t = \frac{\beta_t}{\gamma} \tag{7}$$

We use $\mathcal{R}_t$ for the reproduction number at date t and denote the basic reproduction number by $\mathcal{R}_0$ at the initial stage, when $S_0 = 1$. Beyond the initial $t = 0$, our formulation will allow for $\mathcal{R}_t$ to be affected by policy and by rational individual behavior, as elaborated below in sub-section 2.2. We shall also be discussing the effective reproduction number, defined as:

$$\mathcal{R}_e = S_t\mathcal{R}_t \tag{8}$$

We model the transmission rate β_t as a function of three arguments, using the following formulation:

$$\beta_t = \beta_W - \beta_N \left(1 - \frac{N_t}{N^{SS}}\right)^{\alpha} + \beta_\Lambda \exp\left(-\Lambda t\right) \tag{9}$$

The arguments are motivated as follows:

a. β_W is the transmission rate when the economy is open, i.e., production and employment are not restricted.

b. β_N parameterizes the scale of the decline in transmission as activity falls (decline in $\frac{N_t}{N^{SS}}$, employment relative to its steady state), using a power function with parameter α.

c. $\beta_\Lambda \exp\left(-\Lambda t\right)$ expresses the decline in transmission due to learning over time by individuals.

At time $t = 0$, when $\frac{N_t}{N^{SS}} = 1$ we get:

$$\beta_0 = \beta_\Lambda + \beta_W \tag{10}$$

which is the transmission at the initial stage and corresponds to $\mathcal{R}_0 = \frac{\beta_0}{\gamma}$.

After a period of time, which depends on the rate of decline Λ, individuals change their behavior, and when $\exp\left(-\Lambda t\right) \ll \beta_W$ we get that the transmission rate (and hence $\mathcal{R}_t$) rises with employment:

$$\beta_t = \beta_W - \beta_N \left(1 - \frac{N_t}{N^{SS}}\right)^{\alpha} \tag{11}$$

2.1.2 The Clinical Block

The clinical block describes the clinical progression of the disease and the progression of new cases through the healthcare system, depending on the development and severity of symptoms. We postulate the following. Once infected, a person enters an incubation period, a P state, during which there are no symptoms, lasting for $1/\theta_P$ on average. Following it, a person either remains asymptomatic (O) or develops symptoms (M). Denote the share of asymptomatic cases by η. The others $(1 - \eta)$ develop symptoms, and with probability ξ are hospitalized (H). A given share π of patients become critically ill (denoted X), i.e., develop conditions requiring transition to ICU. Following the literature (see, for example, Kaplan, Moll and Violante (2020) and Brotherhood, Kircher, Santos, and Tertilt (2021)), we specify the death probability in this critical state X as:

$$\delta(X_t) = \delta_1 + \delta_2 \cdot \frac{\mathbf{I}(X_t > \overline{X}) \cdot (X_t - \overline{X})}{X_t} \tag{12}$$

where $\overline{X}$ denotes ICU capacity and $\mathbf{I}$ is the indicator function. The reasoning is as follows. When there is no breach of ICU capacity, the death probability is given by δ_1. Whenever there is an overflow, $\mathbf{I}(X_t > \overline{X}) = 1$, the death probability increases with the risk that a patient will not be provided ICU care when needed. The underlying assumption is that the allocation to ICU is random among all patients in need of it, so the risk to be left out of ICU (for a given

patient) is given by $\frac{(X_t-\overline{X})}{X_t}$. At the limit, the death probability $\delta(X_t \gg \overline{X}, \overline{X})$ is given by $\delta_1 + \delta_2$.

At any stage, a person may recover (C). The clinical block is represented graphically in panel b of Figure 1.

The analytical description of the symptomatic branch is:

$$\dot{P}_t = \beta_t(I_{1t} + I_{2t})S_t - \theta_P P_t \tag{13}$$
$$\dot{M}_t = (1-\eta)\theta_P P_t - \theta_M M_t \tag{14}$$
$$\dot{H}_t = \xi \cdot \theta_M M_t - \theta_H H_t \tag{15}$$
$$\dot{X}_t = \pi\theta_H H_t - \theta_X X_t \tag{16}$$
$$\dot{D}_t = \delta(X_t)\theta_X X_t \tag{17}$$

The parameters θ_P, θ_M, θ_H, and θ_X relate to the average time that passes between the stages of infection, symptoms onset, hospitalization, ICU admission, and death, respectively.

Note that a given person moves through the two blocks simultaneously. They relate to two timescales, the infectiousness profile and the clinical progression, which develop in parallel. Each of the blocks characterizes different properties of an infection case: one identifies whether a given person is infectious and the other identifies the severity of the disease (whether one needs hospitalization, for example). Thus, a person might be infectious (stage I of the infection transmission block) and at the same time still show no symptoms, i.e., be in stage P, the incubation period, of the clinical block. Similarly, a person may no longer be infectious (stage R of the infection transmission block) but still be hospitalized (stage H of the clinical block).

2.2 The Economy

We first describe optimal individual decisions (2.2.1) and then elaborate on the aggregate outcomes (2.2.2).

2.2.1 Consumer-Worker Optimization

In each period, there are two groups of individuals in the economy: the majority who are active and a minority who are inactive because of health reasons.

Active workers. Active workers maximize a utility function, which includes standard utility from consumption and disutility from labor; there is no saving/investment. Additionally and importantly, they respond to the epidemic endogenously. The model is thus related to papers which tie macroeconomic dynamics to epidemiological dynamics, which posit that individual rational economic behavior has two-way connections with disease transmission.[2] Notable COVID-related contributions include Atkeson (2021b, 2022), Atkeson, Kopecky,

[2]This issue was explored long before COVID19; prominent examples include Geoffard and Philipson (1996), Fenichel et al (2011), and Fenichel (2013), Greenwood, Kircher, Santos, and Tertilt (2019), and the surveys by Philipson (2000) and Verelst, Lander, and Beutels (2016).

and Zha (2021), Eichenbaum, Rebelo, and Trabandt (2021), Garibaldi, Moen, and Pissarides (2020), and Krueger, Uhlig, and Xie (2020). An elaborate analysis, emphasizing heterogeneous agents, is offered by Kaplan, Moll, and Violante (2020).

Inactive workers. This group is comprised of the following pools (shares of the population): D_t, deceased; X_t, critically ill; H_t, hospitalized; and ϕM_t, workers with COVID19 symptoms, who do not work because they are isolated. The individuals in these pools, apart from the deceased, get a fixed consumption transfer from the government. This formulation follows a modelling idea of Kaplan, Moll and Violante (2020, see page 28); it assumes that the government has access to a storage technology for final goods and has accumulated a sufficient quantity of goods to provide for the consumption of the afore-cited pools during the pandemic. As a result, their consumption is not part of the flow resource constraint. This assumption simplifies the simulation exercise and has no bearing on its quantitative results as these pools are negligibly small throughout relative to the active population.

The utility function of the active workers is given by:

$$U(c_t, n_t, \dot{D}_t) = u(c_t) - \frac{1}{\omega^n(\dot{D}_t, t)} v(n_t) - \ln \omega^x(\dot{D}_t, t) \tag{18}$$

We define and explain each term in turn:

(i) For consumption we postulate a conventional functional form and parameter value.

$$u(c_t) = \frac{c_t^{1-\zeta_c}}{1-\zeta_c} \tag{19}$$

where ζ_c is the constant relative risk aversion parameter, which we set to 1.

(ii) For labor we postulate a conventional functional form and parameter value.

$$v(n_t) = \theta^{1+\zeta_n} \frac{n_t^{1+\zeta_n}}{1+\zeta_n} \tag{20}$$

and ζ_n is the inverse Frisch elasticity of labor supply, set to 4, in line with the synthesis of micro evidence reported by Chetty et al (2013), pointing to Frisch elasticities around 0.25.

This conventional term is multiplied by $\frac{1}{\omega^n(\dot{D}_t,t)}$ capturing the individual response to the epidemic, in the spirit of modelling by Kaplan, Moll and Violante (2020, see their eqs. 21-22). It expresses an increase in the marginal disutility of labor due to the social interactions component of market work in the times of the epidemic. It is a function of the current daily death rate $\dot{D}_t$, and we assume $1 > \omega^n(\dot{D}_t, t) > 0$, $\omega^n_{ss} = 1$, and $\frac{\partial \omega^n(\dot{D}_t,t)}{\partial \dot{D}_t} < 0$.

(iii) The last term in equation 18 offsets the level shift in utility generated by the marginal utility shifter $\frac{1}{\omega^n(\dot{D}_t,t)}$. We assume $1 > \omega^x(\dot{D}_t, t) > 0$, $\omega^x_{ss} = 1$, and $\frac{\partial \omega^x(\dot{D}_t,t)}{\partial \dot{D}_t} < 0$ so that this term, $-\ln \omega^x(\dot{D}_t, t)$, is positive and increases

in $\dot{D}$. This offset follows Kaplan, Moll and Violante (2020) when computing social welfare. The offset term precludes a big fall in one's own individual utility (and consequently in social welfare which aggregates individual utility) when others die, while the individual undertakes precautionary behavior. It can be interpreted as capturing the added value of precautionary behavior, i.e., the value to the individual herself or himself from engaging in precautionary behavior in the face of the death of others.

Under these restrictions, the utility function becomes:

$$U(c_t, n_t, \dot{D}_t) = \ln c_t - \frac{1}{\omega^n(\dot{D}_t, t)}\theta^5 \frac{n_t^5}{5} - \ln \omega^x(\dot{D}_t, t) \tag{21}$$

The lifetime utility maximization problem of active workers, given the individual discount rate r, is given by:

$$max_{\{c_t, n_t\}} \int_{t=0}^{\infty} e^{-rt} U(c_t, n_t, \dot{D}_t) dt = max_{\{c_t, n_t\}} \int_{t=0}^{\infty} e^{-rt} \left[\ln c_t - \frac{1}{\omega^n(\dot{D}_t, t)}\theta^5 \frac{n_t^5}{5} - \ln \omega^x(\dot{D}_t, t) \right] dt \tag{22}$$

$$s.t. \quad c_t = w n_t \tag{23}$$

Using the budget constraint, the F.O.C implies that individual labor supply of utility-maximizing agents can be written as follows:

$$n_t = \frac{\omega^n(\dot{D}_t, t)^{1/5}}{\theta} \tag{24}$$

We assume the following functional form for the marginal utility shifter $\omega^n(\dot{D}_t, t)$:

$$\omega^n(\dot{D}_t, t) = \left(\omega^x(\dot{D}_t, t)\right)^5 \tag{25}$$

where $\omega^x(\dot{D}_t, t)$ is defined to be

$$\omega^x(\dot{D}_t, t) \equiv (1 - g(\dot{D}_t, t)), \quad g(\dot{D}_t, t) < \overline{g} \quad \forall t, \tag{26}$$

The function $g(\dot{D}_t, t)$ depends on the daily death flow and on time and is bounded from above by $\overline{g}$. We discuss the restrictions on $g(\dot{D}_t, t)$ and its functional form below. We use estimation to undertake empirically-based parameterization of this epidemic-related feedback function, $\omega^x(\dot{D}_t, t)$.

Hence, optimal labor supply and consumption of individuals drop when death rates rise and are given by:

$$n_t = \frac{1}{\theta}\left(1 - g(\dot{D}_t, t)\right) \tag{27}$$

$$c_t = w \cdot n_t = w \cdot \frac{1}{\theta}\left(1 - g(\dot{D}_t, t)\right) \tag{28}$$

The parameter $\frac{1}{\theta}$ in equation (27) represents optimal labor supply in steady state (n_{SS}) without the epidemic. The term $\left(1 - g(\dot{D}_t, t)\right)$ is the endogenous time-varying reduction in the individual labor supply relative to the no-epidemic steady state, due to the rational behavioral response by individuals. In the course of the epidemic, actual labor supply is not necessarily the optimal labor supply given by equation (27), because the government might impose even stricter reductions on activity. Denote the limitation on labor supply mandated by the government by $1 - h(L_t, t)$, where L_t expresses lockdown measures. In that case, actual labor supply will follow the government mandate, and consumption will be set according to the budget constraint $c_t = wn_t$. Therefore, the following inequality should hold true in all periods:

$$n_t \leq \frac{1}{\theta}\left(1 - h(L_t, t)\right) \tag{29}$$

Hence, formally:

$$n_t = \frac{1}{\theta} min\{1 - g(\dot{D}_t, t), 1 - h(L_t, t)\} = \frac{1}{\theta}(1 - max\{g(\dot{D}_t, t), h(L_t, t)\}) \tag{30}$$

$$c_t = w \cdot \frac{1}{\theta}\left(1 - max\{g(\dot{D}_t, t), h(L_t, t)\}\right) \tag{31}$$

2.2.2 Production and Labor

Denote by $\mathcal{P}_t$ the aggregate population of active, representative agents in period t. In the pre-epidemic steady-state: $\mathcal{P}_t = \mathcal{P}_{SS}$. During the epidemic, aggregate employment falls due to people being unable to work because of health reasons. The active population is therefore:

$$\mathcal{P}_t = \mathcal{P}_{SS} \cdot (1 - D_t - X_t - H_t - \phi M_t). \tag{32}$$

The hours of labor supplied by the representative agent in period t, n_t, derived in equation (30), is in daily hours. The aggregate hours worked in period t, N_t, are thus:

$$N_t = \mathcal{P}_t \cdot n_t \tag{33}$$

In the pre-epidemic steady-state, $N_{ss} = \mathcal{P}_{ss} \cdot n^{ss}$. During the epidemic, both aggregate employment $\mathcal{P}_t$ and the intensive margin n_t change, so that:

$$N_t = \mathcal{P}_{SS} \cdot (1 - D_t - X_t - H_t - \phi M_t) \cdot \frac{1}{\theta}\left(1 - max\{g(\dot{D}_t, t), h(L_t, t)\}\right) \tag{34}$$

Therefore, the relative scale of economic activity during the epidemic, aaggregate hours worked by the active population relative to the pre-epidemic steady-state, is given by (noting that $n_{SS} = \frac{1}{\theta}$):

$$\begin{aligned} \frac{N_t}{N_{SS}} &= \frac{\mathcal{P}_{SS} \cdot (1 - D_t - X_t - H_t - \phi M_t) \cdot \frac{1}{\theta}\left(1 - max\{g(\dot{D}_t, t), h(L_t, t)\}\right)}{\mathcal{P}_{SS} n_{SS}} \\ &= (1 - D_t - X_t - H_t - \phi M_t) \cdot \left(1 - max\{g(\dot{D}_t, t), h(L_t, t)\}\right) \end{aligned} \tag{35}$$

The production function of the firm is linear in aggregate hours:

$$Y_t = A \cdot N_t \tag{36}$$
$$Y_{ss} = A \cdot N_{SS} \tag{37}$$

Where the empirical counterpart of A is the average daily output per worker in the pre-epidemic steady-state. The firm maximizes its flow profits w.r.t. employment so:

$$\Pi_t = AN_t - wN_t$$
$$\rightarrow w = A \tag{38}$$

Thus aggregate consumption of active workers equals the aggregate flow output:

$$C_t = \mathcal{P}_t \cdot c_t = \mathcal{P}_t \cdot w \cdot n_t = \mathcal{P}_t \cdot A \cdot n_t = A \cdot N_t = Y_t \tag{39}$$

We normalize to 1 the pre-epidemic steady-state population of representative agents, i.e., $\mathcal{P}_{SS} = 1$.

2.3 Policy Based on Time Restrictions

The new policy, pertaining to the entire population, was introduced in Karin et al (2020), where its epidemiological implications are analyzed extensively. Following an initial lockdown, move to a regime of k days of work and $14 - k$ days of lockdown, every 14 days. On work days, people are released from lockdown with strict hygiene and physical distancing measures on the same k weekdays for everyone. On lockdown days, people are kept away from work places as well as from other public spaces. Epidemiological measures need to be used throughout, including rapid testing, contact isolation, and compartmentalization of workplaces. All strategies respect regular weekends, facilitating application. Table 1 offers a visual summary.

Table 1

Epidemic dynamics using these policies are discussed in detail below, where they are depicted graphically in Figure 4 (see Section 4).

The rationale for the policy is as follows. Cyclical strategies reduce the average value of the reproduction parameter – which will be shown below to capture the progress of the disease – through two effects: time-restrictions and anti-phasing.

The *time-restrictions effect* is a reduction in the time T that an infectious person is in contact with many others, compared to the situation with no lockdown. For example, a 4-day work, 10-day lockdown cycle ($k = 4$) reduces T to $\frac{4}{14}T \approx 0.3T$. The *anti-phasing effect* uses the timescales of the virus against itself. Most infected people are close to peak infectiousness for about 3-5 days,

beginning after a latent period of about 3 days (on average) after exposure. A proper work-lockdown cycle, such as a 4-work 10-lockdown schedule, allows most of those infected during work days to reach maximal infectiousness during lockdown, thus avoid infecting many others. Those with significant symptoms can be infectious for longer, but remain hospitalized, isolated, or quarantined along with their household members, preventing secondary infections outside the household.

As Table 1 shows, we only consider $k \leq 8$ in our analysis of the cyclical strategies. This is because higher values of k imply shorter periods of lockdowns, for example, locking only on weekends. Though similar lockdown policies have been implemented (for example, in India), they do not line up with the epidemiological rationale of the cyclical policies. Furthermore, we find that, in the U.S. context, such extremely open policy tools are hardly consistent with a policy of efficient epidemic suppression. As noted above, online Appendix A provides further details.

2.4 The Planner Problem

The Social Welfare Function. The benevolent planner maximizes discounted social welfare, in expected present value terms. In any given period, social flow welfare is the sum of the agents' flow utilities, less the value of lives lost in that period:

$$W(T_0, T_1, T_2) = \tag{40}$$
$$= \int_{T_V=0}^{\infty} f(T_V) \cdot \int_0^T e^{-rt} \left[\begin{array}{c} \mathcal{P}_{ss} \cdot (1 - D_t - X_t - H_t - \phi M_t) U(c_t, n_t, \dot{D}_t) \\ -\mathcal{P}_{ss} VSL^U \cdot \dot{D}_t \end{array} \right] dt$$

where c_t and n_t are defined in equations (30) -(31), T is the planning horizon, T_V denotes the time till vaccine arrival distributed according to $f(T_V)$, and the term VSL^U denotes the statistical value of life in utility units.

The first term in the square brackets depends on the utility of active workers, from the group $\mathcal{P}_{ss} \cdot (1 - D_t - X_t - H_t - \phi M_t)$, and is given by $U(c_t, n_t, \dot{D}_t)$, where c_t, n_t and $\dot{D}_t$ are defined in (30) - (31) and in 17. The planner assumes that the welfare of inactive agents is zero. Hence, relative to their steady state utility, prior to disease outbreak, there is a social welfare loss for the duration of their inactivity.

The second term in the square brackets is a lost lives value term, not part of the individual utility function. It often features in this context; see, for example, Acemoglu, Chernozhukov, Werning, and Whinston (p.492, 2021), Alvarez, Argente, and Lippi (eq.7 on p. 371, 2021), and Farboodi, Jarosch, and Shimer (eq. 13 on p.13, 2021). It is made up of the product of the aggregate death flow $\dot{D}_t$ and the value of statistical life in utility terms, VSL^U.

The planner takes into account the possibility of a pharmaceutical resolution of the epidemic. We assume that at time T_V a vaccine and a cure are found simultaneously (similar to the assumptions made by Acemoglu, Chernozhukov, Werning, and Whinston (2021) and Alvarez, Argente, and Lippi (2021)). We

assume that after T_V no new cases arise and all inactive workers recover immediately. The waiting time till vaccine/cure introduction is uncertain, and it is distributed according to the probability density function $f(T_V)$, known to the planner. We elaborate on the functional form of $f(T_V)$ and the intuition underlying it in sub-section 2.5 below. Immediately after T_V, the economy moves to the no-epidemic steady state.

The Planner Maximization Problem. The planner takes the individual optimization described in sub-section 2.2.1 as given, and maximizes the afore-cited objective function through the choice of three regime-switching dates: T_0, the start of the initial lockdown, T_1, the date at which the planner switches from initial lockdown to the cyclical strategy, and T_2, the date at which the planner abandons the cyclical strategy and removes all restrictions on economic activity. The lockdown regime L_t changes at dates T_0, T_1, T_2, as described below, and the stringency of lockdowns under different regimes is fixed when the planner decides on the optimal timing T_0, T_1, T_2. We describe the calibration of L_t under different regimes in sub-section 3.2.2 below. The full problem of the planner reads:

$$max_{T_0,T_1,T_2} W(T_0, T_1, T_2) \tag{41}$$

subject to equations (1) -(6), (9), (12) ,(13)-(17), (21), and (30) - (31), where lockdown policy L_t is defined as follows:

$$L_t = \begin{cases} 0 \quad if \quad t \leq T_0 \\ L_L \quad if \quad T_0 < t \leq T_1 \\ L_W = 0 \text{ on open days or } L_L \text{ on closed days} \quad if \quad T_1 < t \leq T_2 \\ 0 \quad if \quad t > T_2 \end{cases} \tag{42}$$

where L_L is the lockdown stringency on "closed" days and $L_W = 0$ on "open" days. We further assume that the process of learning (see the last term in equation (9)) is triggered either by the imposition of lockdown of at least 14 days or by the endogenous response that is significant enough (i.e., $g(\dot{D}_t, t) > L_L$).

Social Welfare Loss. One can compute the social welfare loss in consumption or output terms. We define the flow welfare loss as follows:

$$WL\left(n_t, \dot{D}_t\right) \equiv \widetilde{V}\left(n_{ss}, 0\right) - \widetilde{V}\left(n_t, \dot{D}_t\right) \tag{43}$$

where $\widetilde{V}_t$ is the planner instantaneous utility, $U\left(n_{ss}, 0\right) = \widetilde{V}\left(n_{ss}, 0\right)$ is steady state utility with no deaths, and

$$\widetilde{V}\left(n_t, \dot{D}_t\right) = \ln\left(w \cdot n_t\right) - \frac{1}{5}\left(\frac{n_t}{n_{ss} \cdot \omega^x(\dot{D}_t, t)}\right)^5 - \ln \omega^x(\dot{D}_t, t) - VSL^U \cdot \dot{D}_t \tag{44}$$

We also define the function WL_0 to be the welfare loss function when no disease is present

$$WL_0(n_t) \equiv WL(n_t, 0) \tag{45}$$

Appendix B shows that we can define the inverse function

$$\widetilde{n}_t = WL_0^{-1}(WL_t) \tag{46}$$

This function maps the instantaneous welfare loss, WL_t, to a corresponding hours value, $\widetilde{n}_t$, that if worked in a world with no disease, would have caused this welfare loss. The decline in consumption (in percentage points) corresponding to WL_t is given by

$$CL(WL_t) = \frac{n_{ss} - WL_0^{-1}(WL_t)}{n_{ss}} = 1 - \frac{WL_0^{-1}(WL_t)}{n_{ss}} \tag{47}$$

Equation 47 translates the instantaneous welfare loss WL_t to an instantaneous reduction in consumption, CL_t, in percentage terms. The corresponding PDV value of consumption reduction corresponding to the welfare loss due the disease is given by

$$PDV\_CL(WL_t) = \int_{t=0}^{\infty} \exp(-rt)\, CL(WL_t)\, dt \tag{48}$$

2.5 Modelling Vaccine Arrival Time

The term $f(T_V)$ is the probability density function of the availability of a vaccine at time T_V. This is an important term as it sets the horizon for the problem, acting as a hazard rate for leaving the state of the pandemic. It is an expression of the essential risk and uncertainty embodied in the planner problem. Note that were we to model an arrival time known with certainty, not only would an important real world aspect be removed, but such modelling might create an artifact in the optimal plan. The planner may enable an outbreak shortly before vaccine arrival, relying on the vaccine to eradicate it. Such a plan is not robust to delays in the arrival time. Relative to the interest rate r, expressing time preference, $f(T_V)$ plays the major quantitative role in discounting future streams. The constancy of r makes the planner problem time-consistent, as shown by Halevy (2005). We examine two alternative distributions for $f(T_V)$.

The baseline distribution is the Gumbel distribution, which use is justified by the following logic. We assume that the arrival of the vaccine is a result of simultaneous competition among many firms. The time of arrival is the minimum development time across these firms. Note that over the course of 2020-2022 over 110 vaccines were in clinical trials and dozens more in pre-clinical evaluations. The distribution of arrival time is then well approximated by a Gumbel distribution (see Kotz and Nadarajah (2000)), which is a member of the family of extreme value distributions. Specifically, it is used for modeling the minimum of a sample from many distributions, including exponential, logistic, and normal distributions. Under mild regularity conditions, it is suitable to be a model for a sample minimum even when the distributions from which the

sample is drawn are unknown. In our setting, we remain agnostic about the distributions of vaccine development time by individual firms.

In terms of the model, T_V refers to the time of sufficient vaccination. With logistics, production times, gradual take-up rates, etc. an ex-ante expected 540 days seems reasonable relative to the March 2020 start date of the epidemic in the U.S. [3]This number (540 days) is also the one used by Alvarez, Argente, and Lippi (2021) and Farboodi, Jarosch, and Shimer (2021), and is the middle of the range in Acemoglu, Chernozhukov, Werning, and Whinston (2021).

The cumulative distribution function $G(x)$ of a Gumbel distribution is defined over the real numbers and parametrized by a location parameter μ_G and a scale parameter σ_G :

$$G(x;\mu_G,\sigma_G) = 1 - \exp\left(-\exp\left(\frac{x-\mu_G}{\sigma_G}\right)\right) \tag{49}$$

We anchor the distribution's parameters (μ_G, σ_G), by positing that the mean of the distribution is 540 days, and that the probability of sufficient vaccination before day 360 is only 1%. These assumptions engender two linear equations:

$$\begin{aligned} E(Gumbel\,(\mu_G,\sigma_G)) &= \mu_G - EulerGamma\cdot\sigma_G = 540 \\ Q(Gumbel\,(\mu_G,\sigma_G),q) &= \mu_G + \log\left(-\log\left(1-q\right)\right)\cdot\sigma_G = 360 \end{aligned}$$

where E is the mean and Q is the quantile function. Targeting a mean of 540 and $Q(q = 0.01) = 360$ leads to the solution of $\mu_G = 565.83, \sigma_G = 44.74$.

As an alternative we examine the exponential distribution, reflecting a Poisson process for vaccine arrival, at a fixed rate for any given day. This has been used by Acemoglu, Chernozhukov, Werning, and Whinston (2021), Alvarez, Argente, and Lippi (2021), Farboodi, Jarosch, and Shimer (2021), and Jones, Philippon, and Venkateswaran (2021). Its drawback is that it has a mode of zero, which is implausible in the case of vaccine development. We calibrate the parameter of the exponential distribution to $1/540$, so that it has the same mean waiting time of 540 days as in Gumbel distribution.

Figure 2 illustrates the resulting calibrated probability density functions. The Gumbel is shown by the solid line and the exponential by the dashed line.

Figure 2

The Gumbel distribution has an asymmetric bell-shaped form, with mode around 540 days, and a rather long left tail. The density drops quite fast after 540 days. The exponential distribution has the desired mean expected waiting time, 540 days, but the implied probability density is strictly decreasing, implying that the first day of the epidemic is the most likely date of vaccine development. This property of the distribution is highly counter-intuitive. However, assuming the exponential distribution is convenient because it fits in smoothly

[3]We have used 540 days in work on simulating this model since the summer of 2020. Actual developments turned out broadly consistent with this number.

with the exponential discount factor which is frequently used in dynamic optimization problems in Economics. In Appendix B we compare the use of Gumbel and Exponential distributions as the basis for an optimizing planner, and show that the welfare loss in using the Exponential is higher.

2.6 Benchmarks

We shall compare the results of simulating the model, calibrated for the U.S. economy, to the following benchmarks:

(i) and (ii) The polar cases of no policy intervention (i.e., no lockdown) or full lockdown till vaccine arrival.

(iii) The case whereby the duration of lockdown is set optimally. This is essentially the case of $k = 0$, i.e., no open days within a cyclical setting, and we shall denote it Optimal Lockdown.

(iv) A theoretical path trying to mimic real-world rationale by re-interpreting the planner problem as choosing thresholds for lockdown policy in terms of the critically ill, X. The first threshold defines a level X_0 whereby if $X_t > X_0$ an initial lockdown is imposed. Subsequently, a second threshold defines a level X_1 whereby if $X_t < X_1$ lockdown is released. Finally, a third threshold defines a level X_2 whereby if $X_t > X_2$ lockdown is re-imposed. The planner chooses the three thresholds optimally. The logic is that the first eruption of the disease is different from later eruptions, since the initial learning period has not yet occurred, and the endogenous response to death lags the infection. Therefore, X_0 allows the planner the freedom to lock earlier or later in the phase of initial eruption, while X_2 enables the planner to lock at a different threshold for later eruptions. The release threshold X_1 is the same throughout. Note that this strategy leads to recurrent lockdown and release policies, and, that the planner here is not as constrained as in the case of the cyclical strategies, where we have allowed for only three optimal points in time to be chosen.

These four cases are compared to six cyclical strategies, which use $k = 3, 4, 5, 6, 7, 8$.

In Section 6 we compare the model to the actual experience of the states of New York and Florida.

3 Calibration and Solution Methodology

We calibrate the model to fit the U.S. economy, which was badly hit by COVID19. Throughout we work in daily terms. In Section 6, we discuss the methodology and calibration values used for the analysis of two specific states in the U.S.

3.1 Calibration of the Epidemiological Model

In Table 2, we present the relevant parameter values for the two blocks, where we rely on sources in the epidemiological and medical literatures published in Science, Nature, the Lancet, and JAMA, as detailed in the table's notes.

Table 2

3.1.1 The Infection Transmission Block

For the duration numbers of the latency period $(1/\sigma)$ and the infectiousness period $(1/\gamma)$ we rely on studies that have appeared early on in the COVID19 pandemic and were published in Science; see Tian et al (2020) and Li et al (2020). These studies were co-written by university researchers from China (Tsinghua, Hong Kong, and others), from the U.S. (Harvard, Princeton, Columbia, Penn State, UC Davis, and NIH), and from the U.K. (Imperial, Oxford, and Southampton). Their findings are confirmed by studies on infector-infectee pairs; see He et al. (2020) and Ma et al. (2020). A number of papers (Tindale et al (2020), Kong et al (2020), and Ren (2021)) highlight the fact that a significant part of disease transmission happens before the onset of symptoms. This implies that the latent period is shorter than the incubation period, which is usually 5-6 days (see the review in Bar-On et al (2020) and the references therein). The latter appears within the clinical block to which we turn now.

3.1.2 The Clinical Block.

The value for the duration till death is given by $\frac{1}{\theta_P}+\frac{1}{\theta_M}+\frac{1}{\theta_H}+\frac{1}{\theta_X}$ and is set at 19.5 days based on CDC estimates. We use $\overline{X}=\frac{58{,}094}{329.529*10^6}=1.8\times10^{-4}$ based on an estimate of $58,094$ ICU beds by the Harvard Global Health Institute.

The implied Infection Fatality Rate (IFR) is given by $IFR=\xi\cdot\pi\cdot\eta\cdot\delta_1$. Estimates of the Imperial College COVID19 Response Team (2020) and the meta-analysis findings of Meyerowitz-Katz and Merone (2020) put IFR at 0.8%. Meyerowitz-Katz and Merone (2020) state: "Based on a systematic review and meta-analysis of published evidence on COVID-19 until July 2020, the IFR of the disease across populations is 0.68% $(0.53\%-0.82\%)$. However, due to very high heterogeneity in the meta-analysis, it is difficult to know if this represents a completely unbiased point estimate. It is likely that, due to age and perhaps underlying comorbidities in the population, different places will experience different IFRs due to the disease. Given issues with mortality recording, it is also likely that this represents an underestimate of the true IFR figure." Using this number and the numbers for ξ, π, and η in Table 2, we derive $\delta_1=0.5$. We then calibrate $\delta_2=0.5$ to capture the fact that, with extreme loads on the public health system, the probability to die increases to 1 for each patient in need of an ICU bed (see the reasoning in sub-section 2.1 above).

3.2 Calibration Based on Estimation

We employ daily U.S. data to estimate key relations and use the point estimates to calibrate the model.

3.2.1 Data

The data series used are daily deaths, daily employment, lockdown measures, and the derived transmission rate. Appendix C elaborates on data definitions and sources. Figure 3 plots these four variables.

Figure 3

The transmission rate falls rapidly till early April 2020; it then rises somewhat till June 2020 and subsequently fluctuates around a fairly stable level. The disease is represented by the daily death series, where a big surge starts the first wave in March 2020 and where the decline starts in late April 2020; a second wave peaks in January 2021. Employment falls rapidly to a low of 80% of its pre-pandemic level in mid April 2020 and recovers, first rapidly and then slowly, though not all the way to its pre-pandemic level. Policy is shown by the weighted lockdown stringency index, which rises to a high level by the last third of March 2020. It subsequently drops in June 2020 and stays constant except for a rise in part of November 2020.

3.2.2 Dynamics of Transmission and the Reproduction Parameter

We estimate equation 9, as reported in panel a of Table 3

Table 3

The estimates imply the following. When $\frac{N_t}{N^{SS}} = 1$ i.e., the economy is not locked and there are no sick or dead, at time $t = 0$:

$$\beta_0 = \beta_\Lambda + \beta_W = 0.339 + 0.376 = 0.715$$

and so $\mathcal{R}_0 = \frac{\beta_0}{\gamma} = 2.86$

Given the estimated rate of decline, $\Lambda = 0.12$, in a little less than a month individuals adjust their behavior to the presence of the disease; subsequently, when $\exp(-\Lambda t) \ll \beta_W$ we get:

$$\beta_t = \beta_W - \beta_N \left(1 - \frac{N_t}{N^{SS}}\right)^\alpha$$

This implies β_t drops endogenously below β_W as a function of employment, yielding reproduction parameter $\mathcal{R}_t$ variation between 1.5 and 0.8.

3.3 Calibration of the Economic Model

Discounting. We posit a 4% annual discount rate ($r = 0.04$), converted to daily terms (used by individuals and consequently by the social planner).

The value of ϕ. As in Glover, Heathcote, Krueger, and Rios-Rull (2020), we assume that anyone who has any symptoms self-isolates and does not work ($\phi = 1$).

The endogenous response, lockdowns, and employment.

In order to calibrate other values appearing in sub-section 2.2 we proceed as follows.

Without restrictions, equation 30 would allow employment to drop very significantly. This can even reduce employment to levels below what is usually regarded as essential employment plus work from home. Empirical estimates

for the U.S. indicate that the minimum employment level under the most stringent lockdown measures was around $0.65 - 0.70$ of full employment (see Blau, Koebe, and Meyerhofer (2021) and Gregory, Menzio and Wiczer (2020)). We therefore calibrate this level of employment to be 0.68 and set $\overline{g} = 0.32$.

We postulate that the functions $g(\dot{D}_t, t), h(L_t, t)$ are given by:

$$\begin{aligned} g(\dot{D}_t, t) &= \kappa_t \dot{D}_t \quad (50) \\ h(L_t, t) &= \varkappa_t L_t \quad (51) \end{aligned}$$

As discussed above, there is an overlap of compliance with lockdown and the endogenous response, so we use the maximal response. The variables $\varkappa_t$ and κ_t express the idea that both endogenous individual response and compliance with lockdown are modelled with time decay f_t. We use the functional form proposed by Atkeson (2021b, 2022) as follows:

$$\begin{aligned} f_t &= normal\_cdf\left(\frac{t-\mu_f}{\sigma_f}\right) \quad (52) \\ \varkappa_t &= \varkappa\left(1-(1-\varphi_\varkappa)\cdot f_t\right) \quad (53) \\ \kappa_t &= \kappa\left(1-(1-\varphi_\kappa)\cdot f_t\right) \quad (54) \end{aligned}$$

where $normal\_cdf$ is the CDF of the normal distribution, $\varkappa_t$ and κ_t are the time-varying parameters of the effects of compliance lockdown and individual response on employment, respectively, and the parameters $\mu_f, \sigma_f, \varkappa, \varphi_\varkappa, \kappa$ and φ_κ are to be estimated.

The resulting estimating equation is given by:

$$\frac{N_t}{Nss} = 1 - \max(\varkappa_t L_t, \kappa_t \dot{D}_t) + \varepsilon_t \quad (55)$$

We non-linearly estimate equation 55 using data on $\frac{N_t}{Nss}$, L, and $\dot{D}_t$ in the period from March 1, 2020 to February 28, 2021. The results are reported in Table 3b. We note that L_L is calibrated to be the highest share of workers who did not work during the course of the disease in the U.S. i.e., 0.20.

Employment, Wages, and the Utility Function.

For the planner problem and the simulations we further need to calibrate θ and A. To do so we use two U.S. data points, as do Eichenbaum et al (2021, pp.5162-3): the representative person works 28 hours per week reflecting the average number of hours worked from the Bureau of Labor Statistics 2018 ATUS and earns an annual income of $58,000, using the 2019 estimate from the U.S. Bureau of Economic Analysis.

Thus, pre-epidemic, which we call steady-state (SS), when $g(\dot{D}_t, t) = 0$ we get, converting weekly hours to daily terms:

$$\begin{aligned} n^{SS} &= \frac{1}{\theta} \\ \theta &= 1/4 \quad (56) \end{aligned}$$

In the aggregate, no-epidemic steady-state: $\mathcal{P}^{SS} = 1$, and $N^{SS} = \mathcal{P}^{SS} \cdot n^{SS} = 4$.

Using daily income W and daily hours, the hourly wage is:

$$w = \frac{W}{n^{SS}} = \frac{\frac{58000}{365}}{4} = 39.73 \tag{57}$$

We use equation (38) and set $A = w$.

Value of Statistical Life.

The planner objective includes the term $\mathcal{P}^{SS} \cdot \dot{D}_t \cdot VSL^U$, where VSL^U is the value of statistical life. We determine its value and show how it fits in the social welfare function.

The central estimate in Hall, Jones, and Klenow (2020) for the monetary value of statistical life lost to COVID19, VSL^{USD}, is 3.81 million USD, based on the EPA estimate of 270,000 USD per year and the authors' estimate of 14.1 years of remaining life on average. For robustness, we look at two sets of alternative values estimates in sub-section 5.3 below.[4]

To include these values in the social welfare function, we apply an oft-used methodology (see, for example, Farboodi et el. (2021, p.16)), as follows: denote the Value of Statistical Life in utility terms by VSL^U, so that the event of death in the model is associated with utility loss of VSL^U. Individuals are indifferent between paying $SHARE_C$ of their flow consumption and avoiding the risk ε of losing VSL^U, and not paying $SHARE_C$ of their flow consumption and carrying the ε risk of losing VSL^U. Given the no-epidemic steady-state utility, this logic means that VSL^U should satisfy the following indifference condition:

$$\frac{\ln c_t - \theta^5 \frac{n_t^5}{5}}{r} - \varepsilon VSL^U = \frac{\ln\left((1 - SHARE_C)c\right) - \theta^5 \frac{n_t^5}{5}}{r} \tag{58}$$

where

$$SHARE_C = \frac{\varepsilon VSL^{USD} \times r}{\frac{C^{USD}}{365}} \tag{59}$$

The representative agent would be willing to pay $SHARE_C$ so as not to lose VSL^U with an ε risk of death; the payment, $SHARE_C$, is given by equation 59, paying $\varepsilon VSL^{USD} \times r$ each day, where r is the daily discounting rate is r.

Assuming $SHARE_C \ll 1$ we get $-\ln(1 - SHARE_C) \simeq SHARE_C$ and using our modelling of $C = Y$ (which we have taken to be 58,000 USD), we get:

$$\begin{aligned} \varepsilon VSL^U &= \frac{SHARE_C}{r} = \frac{\frac{\varepsilon VSL^{USD} \times r}{\frac{Y^{USD}}{365}}}{r} \\ VSL^U &= \frac{VSL^{USD} \times 365}{Y^{USD}} \end{aligned} \tag{60}$$

[4] In Section 2.2 of Appendix B we delineate an elaborate procedure to get such VSL estimates using a number of data sources, including Greenstone and Nigam (2020), and taking into account age groups, finding very similar numbers.

Thus the VSL^U value we get is 23,977 for the baseline VSL^{USD} value of 3.81 million USD.

4 Results

We present the results for the baseline calibration and explore some variations in the next section. Section 2 of Online Appendix C delineates the methodology of the simulations.

The optimizing planner chooses how long to wait till first lockdown (T_0), when to start implementing a cyclical strategy (T_1), and when to release completely (T_2), for each instrument, namely for each given k. Optimal timing is based on probability-weighted scenarios for vaccine arrival over the horizon (T) of two years. According to the vaccine arrival time distribution that we assume, the probability that it will take more than two years to introduce the vaccine is practically 0. In the simulations, vaccine arrival is actually realized on day 540, at its arrival time in expectation, using the afore-discussed Gumbel distribution.

We present the results for the benchmarks discussed in sub-section 2.6 above – no intervention, full lockdown, optimal duration lockdown, and a thresholds strategy on X – and the cyclical strategies. Table 4 reports the planner's optimal timing T_0, T_1, T_2, the resulting values of social welfare loss in terms of utility and in terms of consumption (both delineated in the table's notes), loss of annual GDP (in PDV, per annum terms, evaluated over two years), and the cumulative number of deaths, per 1 million people.

Figure 4 shows the time evolution of key series for three benchmarks (to avoid clutter we omit the optimal lockdown case) and three of the cyclical strategies ($k = 4, 5, 8$). The series plotted are as follows: flow deaths ($\dot{D}_t$), the endogenous response $\kappa_t \dot{D}_t$, the effective reproduction parameter $\mathcal{R}_e$, the employment level relative to its pre-epidemic steady state $\frac{N_t}{N_{SS}}$, and the flow (first difference) welfare loss in consumption terms $PDV\_CL(W_t)$, as computed from equations (47)-(48). For clarity of presentation, the series (except for the endogenous response) are smoothed and what is presented is a 14 days moving average.

Table 4 and Figure 4

Table 4 and Figure 4 show that the results can be characterized as follows.

The *cyclical strategies with low k* ($k = 3, 4$) lock the economy immediately for 14 days and then implement the cyclical strategy for an extended period of time. Because open days are relatively few, these strategies keep the epidemic under control. Flow deaths ($\dot{D}_t$) and the stock of cumulative deaths (D) are very low, and $\mathcal{R}_e$ is kept at 1 for most of the time – see the $k = 4$ case in Panel A of Figure 4. As a consequence, the endogenous response $\kappa_t \dot{D}_t$ is low as well for most of the time, peaking at 1% of the work force during the initial breakout of the epidemic until it is contained.

During the prolonged cyclical phase, with relatively few open days, employment averages around 85% of its steady state level; GDP loss is around $20\% - 21\%$ in PDV per annum terms evaluated over two years. Welfare loss, in terms of the PDV over the two year period, is around $33 - 35$ in utility terms (to be compared to other strategies below) and is around $22\% - 23\%$ in annual consumption terms. In flow terms, the loss is for most of the time around 15% of steady state consumption.

The *cyclical strategies with higher k* $(= 5, 6, 7, 8)$ lock the economy immediately for an extended period of time; the higher the k, the longer the initial lockdown period. They then implement the cyclical strategy up to vaccine arrival. During the initial lockdown period, starting at T_0, $\mathcal{R}_e$ is below 1, but when the cyclical regime is in effect, $\mathcal{R}_e$ is above 1, and the higher the k, the higher is $\mathcal{R}_e$. Flow deaths ($\dot{D}_t$) rise; see, for example, the $k = 8$ case in Panel a of Figure 4. Consequently, the endogenous response $\kappa_t \dot{D}_t$ rises as well enhancing the efficacy of cyclical tools and driving the effective reproduction parameter $\mathcal{R}_e$ towards 1.

In the case of $k = 5$, $\mathcal{R}_e$ converges to just above 1 almost immediately with the start of the cyclical phase, while for higher k values vaccine arrival occurs before this convergence has been completed.

Looking at the $k = 8$ case in Panel a of Figure 4 we see the following: employment is low, at 80% during the initial lockdown, and then jumps to around 90% at the beginning of the cyclical phase. It gradually declines thereafter, due to the endogenous response. The loss of GDP and welfare is higher relative to the low k ones: GDP loss is 24% as compared to $20\% - 21\%$ in PDV per annum; welfare loss is 40 as compared to $33 - 35$ in PDV terms (over two years), and 26% as compared to $22\% - 23\%$ in annual consumption terms. In flow terms, welfare loss is quite stable at around 20% of steady-state consumption during the year-long initial lockdown, it then drops with the transition to the cyclical regime, and subsequently gradually rises to around 16% due to the increase in the death toll, until vaccine arrival.

The results for three benchmarks, discussed in sub-section 2.6 above, to which we compare the afore-going cyclical policies, are as follows.[5] Note, that the first two are non-optimizing, extremal benchmarks.

The no policy intervention case has the disease erupt: flow deaths ($\dot{D}_t$) and the stock of cumulative deaths (D_t) are the highest across all the policies examined here; total deaths are higher by a factor of almost 60 relative to the $k = 3$ or $k = 5$ cases. There is a strong endogenous response and employment falls to its lower limit, 68% of the steady state level. This endogenous response and the fast erosion of the Susceptibles pool, S_t, bring the effective reproduction number $\mathcal{R}_e$ to unity in less than three months. GDP loss is relatively low, at around 10% in PDV per annum terms evaluated over two years, and results solely from the endogenous precautionary behavior of individuals. In PDV terms, the cumulative welfare loss is extremely high, at around 69 (compared to

[5]While here we compare to theoretical benchmarks, note that in Section 6 below we directly compare the model results to two actual U.S. cases – New York State and Florida

33-40 in the cyclical strategies), which amounts to 36% of annual consumption (compared to $22\% - 26\%$ for the cyclical strategies). In flow terms, the welfare loss surpasses 50% of steady state flow consumption during the initial eruption and fluctuates between 10% and 30%of steady state consumption thereafter.

The full lockdown case has the disease under control as it entails an immediate lockdown, remaining in place until vaccine arrival. It leads to a very low number of deceased, 21 people per million. As it leads to a decline of employment of 80% of its steady state value, it has a substantial cost, at almost 29% of annual GDP in PDV terms over two years. This output loss translates to a welfare loss: in PDV terms the V loss is almost 47, as compared to $33 - 40$ in the cyclical strategies, and is 29% in annual consumption terms. In flow terms, it is around 19% of steady state consumption for most of the time.

The thresholds policy case follows a prevalent policy rationale, though this is not the policy actually implemented anywhere. The planner optimally chooses thresholds for lockdown policy in terms of ICU hospitalizations, X, and keeps the epidemic under control. Flow deaths ($\dot{D}_t$) and the stock of cumulative deaths (D) are relatively low, and $\mathcal{R}_e$ fluctuates between 0.76 and 1.40 most of the time. The endogenous response $\kappa_t \dot{D}_t$ is low for much of the time, except for an initial spike. With the recurring lockdowns, employment fluctuates between 80% and 100% of its steady state level; GDP loss is around 25% in PDV per annum terms evaluated over two years. In terms of PDV welfare loss, the V decline is around 38 in utility terms, compared with $33 - 34$ in the low k cyclical strategies, and is 25% in annual consumption terms, compared with $22\% - 23\%$ in the low k cyclical strategies. In flow terms, the social welfare loss fluctuates between 4% and 20% of steady state flow consumption.

The optimal lockdown case ($k = 0$) features a long lockdown beginning on day 12 and results in outcomes that lie between the two extremal benchmarks and the thresholds policy case in terms of social welfare loss (see row (iv) in Table 4). It has a lower death toll relative to the thresholds policy with a higher GDP loss. It is clearly inferior to the cyclical strategies.

Overall, the emerging picture is that the extremal benchmarks yield high welfare losses. This is so because policy is either non-existent or non-optimal. All other strategies have lower welfare losses because they optimally balance the cost of deaths and economic costs. A policy using thresholds on X achieves substantial improvement in welfare terms but is still inferior to the low k strategies (with $k \leq 6$). The cyclical policies obtain better welfare results within a narrow range. Hence the different cyclical policies perform the best, within the set of policies examined, but between them there is relatively little difference. In Section 6 below, we compare the cyclical strategies with real world results for two states, New York and Florida.

5 Exploring Planner Policies

While the preceding section presented the baseline results, in this section we analyze the mechanism, its implications, and robustness. First, we study the

underlying mechanism, exploring the rationale for the planner optimal decisions (sub-section 5.1). Subsequently, we evaluate the cyclical policies by comparing them to the alternative benchmark policies using a plot of the policy possibilities frontier (5.2). Finally, we study variations in key parameters (5.3).

5.1 The Mechanism

The underlying mechanism is as follows. The progression of the epidemic can be classified by the *effective* reproduction number $\mathcal{R}_e$, which depends both on the current reproduction number $\mathcal{R}_t$ and on the current fraction of susceptibles S_t, i.e., $\mathcal{R}_e = \mathcal{R}_t \cdot S_t$, where $\mathcal{R}_t$ reflects the current policy intervention regime and/or the endogenous behavioral response of individuals to the epidemic. A low $\mathcal{R}_e$ is achieved (i) following an extensive exposure of the population to the virus (engendering a low S_t), (ii) by the endogenous response of individuals who decrease their activity, thereby reducing $\mathcal{R}_t$, (iii) by imposing stringent policy restrictions to curb virus spread, thereby lowering $\mathcal{R}_t$. The following classification is useful:

(i) When $\mathcal{R}_e < 1$, the epidemic is suppressed and the number of newly infected people declines with time.

(ii) When $\mathcal{R}_e = 1$, the disease is stable and an outbreak (i.e., a spurt of disease growth) is no longer possible, though susceptibles still do get infected at some slowly declining rate.[6]

(iii) When $\mathcal{R}_e > 1$, the amount of people who are infected daily grows, some of whom become ill, hospitalized, and may eventually die. However, this case is not sustainable over time: the rising daily death toll elicits an endogenous response from individuals, causing them to be cautious and to restrict their economic activity, which in turn reduces the infection transmission rate and thus reduces $\mathcal{R}_e$. Thus the endogenous response provides for a negative feedback mechanism, which prevents the disease from spiralling out of control.

We can now formulate the outcomes of the optimal planning problem in these terms. The outcomes presented in the preceding section basically follow one of two basic paths.

Exogenous containment. This path implies that $\mathcal{R}_e$ is kept below or around 1 throughout most of the planning period using stringent restrictions, while preserving the pool of the susceptibles intact to a large extent. This path requires strong suppression measures to be imposed for long periods of time. These measures either reduce the epidemic or keep it growing at a very slow pace. The costs in terms of foregone output are relatively high, but the death toll is low.

Endogenous containment. This path implies that there is a reduction in $\mathcal{R}_e$ to around 1 through the endogenous response of individuals, while policy interventions are loose or short-lived. Since this path involves less prolonged and delayed interventions, it is cheaper in terms of the loss of output, while the

[6]There is a decline in the rate of infection since the number of susceptibles S_t is declining with each person infected.

ensuing death toll is inevitably higher (relative to the *exogenous* containment path).

These two policy paths reflect planner choices in relation to the fundamental trade-off between economic costs and death tolls in managing the epidemic. The resolution of the trade-off, the optimal policy choice, depends on a number of factors: the extent to which economic activity can be maintained in lockdowns, the fatality rate of the virus, the scope of the endogenous response of individuals to death, and the value of statistical life. Importantly, it depends on the type of policy instruments available to the planner. It turns out that when cyclical strategies are in the policy toolkit, the fundamental trade-offs can be softened in a way that allows achieving lower economic costs and/or lower death tolls, all while waiting for vaccine arrival. The underlying rationale behind the social welfare improvement engendered by the cyclical strategies is that they average out k working days and $(14-k)$ lockdown days and therefore reduce $\mathcal{R}_t$. The approximation of the average $\mathcal{R}_t$, to be denoted $\mathcal{R}_a$, is given by:[7]

$$\mathcal{R}_a(k) \simeq \frac{(14-k)\cdot \mathcal{R}_L + k\cdot \mathcal{R}_{W_t}}{14} \tag{61}$$

where $\mathcal{R}_L$ is the the reproduction number on days of lockdown, given by:

$$\mathcal{R}_L = \frac{\beta_W}{\gamma} - \frac{\beta_N}{\gamma}\left(L_L\right)^{\alpha} \tag{62}$$

This is so under the assumptions that $L_L > \kappa_t \dot{D}_t$ and that the economy has passed the initial stages of the disease so $\exp\left(-\Lambda t\right) \ll 1$.

$\mathcal{R}_W$ is the the reproduction number on open days (no lockdown) and is given by:

$$\mathcal{R}_{W_t} = \frac{\beta_W}{\gamma} - \frac{\beta_N}{\gamma}\left(\kappa_t \dot{D}_t\right)^{\alpha} \tag{63}$$

This is so under the assumption that the economy has passed the initial stages of the disease so $\exp\left(-\Lambda t\right) \ll 1$.

An effective lockdown policy measure L_L, should be set such that $\mathcal{R}_L < 1$ i.e. $L_L > \left(\frac{\beta_W-\gamma}{\beta_N}\right)^{1/\alpha}$.[8]

Combining equations (61),(62), and (63) yields:

$$\mathcal{R}_a(k,\dot{D}_t) \simeq \frac{\beta_W}{\gamma} - \frac{\beta_N}{\gamma}\left(\frac{k}{14}\left(\kappa_t \dot{D}_t\right)^{\alpha}\right) - \frac{\beta_N}{\gamma}\left(1-\frac{k}{14}\right)\left(L_L\right)^{\alpha} \tag{64}$$

The last equation shows that the reduction in the reproduction number (the terms with a minus sign) depends on a weighted average of lockdown measures and the endogenous response to death flow numbers.

[7] The true average is not exactly a linear function of $\mathcal{R}_W$ and $\mathcal{R}_L$ (due to the anti-phasing effect and non-linearities of disease dynamics) and so this is a first order approximation.

[8] The estimates for the relevant parameters satisfy this condition.

We now make the connection between the afore-cited concepts: the effective reproduction parameter, $\mathcal{R}_e$, types of containment (*exogenous* and *endogenous*), and the average reproduction parameter, $\mathcal{R}_a$.

The basic classification into containment types is made under the assumption that the death toll is low $\left(\dot{D}_t \simeq 0\right)$.

If $\mathcal{R}_a(k,0) \leqslant 1$, the cyclical strategy is based on *exogenous* containment, and the disease is contained as long as the cyclical policy is in effect. This is so because when $\dot{D}_t \simeq 0$ and $R_a(k,0) \leqslant 1$, then $R_e \leqslant 1$ holds true throughout, the disease does not grow, and death rates remain suppressed so that the endogenous response plays no role.

If $\mathcal{R}_a(k,0) > 1$, *endogenous* containment takes place. The disease grows, triggering an endogenous response that drives $R_a(k,\dot{D}_t)$ down until $R_e = 1$ and the disease is subsequently contained at some fixed level.

Note that all optimal cyclical strategies are based on restricting the size of the epidemic, so by the time of vaccine arrival, only $1\% - 3\%$ of the population is exposed to the virus. In other words, the policy-maker never relies on the erosion of the Susceptibles pool, S_t, as a means to drive the effective reproduction number $\mathcal{R}_e$ down.

From the parameters estimated for the U.S., one can see that the low-k strategies ($k = 3,4$) are used to achieve *exogenous* containment, using a very early lockdown phase followed by an extremely prolonged cyclical stage. Exogenous containment is possible since the average reproduction parameter $\mathcal{R}_a$ implied by these strategies, even without an endogenous response, is low, and so they achieve an effective $\mathcal{R}_e$ below unity. Crucially, they can bring down the infection while not closing down the economy completely.

The $k = 5$ strategy is based on *endogenous* containment, following an initial lockdown period of just above 3 months. However, the endogenous response is not quantitatively large: since $\mathcal{R}_a$ is only a little over 1, as the disease starts to grow, the endogenous response immediately brings $\mathcal{R}_e$ to 1, keeping the disease, and death rates, at low levels ever since.

The less stringent strategies ($k = 6,7,8$) are used to achieve *endogenous* containment as well. These strategies use much longer initial lockdown periods (3 – 5 months), before moving to the cyclical phase. After initial suppression, using the cyclical strategies, the disease grows slowly, and with its rise, the endogenous response brings $\mathcal{R}_e$ back to 1. These dynamics can be seen in Figure 4 above. In Section 3 of online Appendix C we report the R_a and S_t values associated with these different policies.

5.2 The Policy Possibilities Frontier

As discussed above, there are two major ways to deal with the epidemic, *exogenous* and *endogenous* containment. The trade-offs involved are most easily seen in a two-dimensional graph, that maps the outcome obtained under each instrument on two axes, the death toll per million people and the value of lost output in annual GDP terms. One can trace out a policy possibilities frontier using this graphical representation. Figure 5 presents several variations of this

frontier.

Figure 5

Panel a of the figure shows the frontier plot using the baseline values, discussed in Section 3 and presented in Table 4 and Figure 4. Thus it shows the cyclical strategies as well as the benchmark strategies, discussed in sub-section 2.6. The analysis is conditional on the baseline $VSL^{USD} = 3.81M\$$. The two extreme benchmarks of full lockdown (labelled 'lock till vaccine' arrival) and no intervention (labelled 'do nothing') are represented by two extreme points on the graph, with huge output or death toll, respectively, well beyond the frontier. The benchmark optimal duration lockdown policy (labelled 'lockdown only') lies above the frontier too, as does the thresholds strategy benchmark. All cyclical strategies are located at the left part of the graph. The figure clearly shows that the use of cyclical strategies brings about a very substantial improvement in outcomes relative to the two extremes of no intervention or full lockdown (as also seen in the values reported in Table 4). Compared to the optimal thresholds strategy, the cyclical strategies provide significant improvement too.

In the zoomed-in graph, the cyclical strategies trace out two linear frontier curves, of the two types of containment. The strategies marked in green follow *exogenous* containment policies. These are low-k strategies with just a few days open each fortnight. They trade off a higher cost of lost output for a lower death toll. They are on the frontier marked in green, nearer the origin. The other cyclical strategies, marked in red $(k = 6, 7, 8)$, are not as powerful in suppressing the epidemic, as more open days are allowed every fortnight and therefore rely on *endogenous* containment. They are represented by the frontier schedule in red, further away for the origin.

Notably, the outcome of the $k = 5$ cyclical strategy, which belongs to the *endogenous* containment set, is located in the vicinity of the *exogenous* containment strategies outcomes. This is so as it achieves a low R_a (1.05) and is superior to the other *endogenous* containments strategies. With this exception, under the baseline calibration, the outcomes achieved by *exogenous* containment strategies are superior to the outcomes of *endogenous* containment strategies. The former limit the economic activity of agents, using the cyclical strategy so that the disease does not erupt. The latter strategies rely on the reaction of people to the death toll in order to limit economic activity. In order to limit the death toll, these strategies rely on a longer initial lockdown period, which is more costly in terms of social welfare loss.

5.3 Variations in Key Parameters

We turn to examine robustness of our results and look at variations in key parameter values. We continue using frontier terminology and plots.

First, we look at variations in the Value of Statistical Life. Varying the planner's preferences does not alter the big picture: the planner opts for a low death toll, and *exogenous* containment is preferred to *endogenous* containment. In the case of the *exogenous* containment strategies $(k = 3, 4)$ as well as in the case of

the $k = 5$ strategy, the planner is near the limit of the possibility to minimize death, so the optimal planning choice does not change much with the change in value of VSL. In the case of the *endogenous* containment cyclical strategies ($k > 5$) the change of VSL translates into a movement along the frontier with an almost constant slope. A rise of VSL causes the planner to lengthen the initial lockdown period (an increase in $T_1 - T_0$), raising the loss of GDP and reducing death. A lower VSL causes the planner to shorten the initial lockdown period, which translates into a lower GDP loss and a rise in the death toll. We present the results in full in sub-section 2.2.3 of Appendix B.

Second, the cited trade-offs also depend on the infection fatality rate. Panel b in Figure 5 and Table 5 present the results with the alternative IFR values of 0.6%. and 1.2%**.**

Table 5

A lower IFR means a less lethal disease so better outcomes can be achieved by the planner and thus welfare loss, compared to the baseline, is always lower. This enables the planner to shorten the initial lockdown period, which, combined with the lower IFR, leads to a lower death toll, lower GDP loss, or both. A higher IFR means that the disease is more lethal, and thus welfare loss compared to the baseline is higher. This leads the planner to lengthen the initial lockdown period, and with the higher IFR, there is either a higher death toll, a higher GDP loss, or both.

The most conspicuous feature of Figure 5d is that low- k strategies fare much better, whatever the IFR. For all cyclical strategies, a higher IFR, usually translates into a upward-rightward movement (moving from black to blue points), with an increase of both death and output loss. A lower IFR usually translates into a movement downward-leftward (moving from black to green points), with a decrease in death and output loss.[9]

We conclude that the finding of low-k, exogenous containment strategies being superior is robust to the parameter value variations examined.

5.4 Discussion

What is the broader picture emerging from the analysis? Even in the absence of any restrictions, two mechanisms lead to output loss. The first is the direct effect generated by infected people who cannot work. The second, and more significant one, is that individuals self restrict their economic activity in order to avoid infection. In our analysis output loss without policy intervention was shown to be significant. This demonstrates the critical role of the endogenous individual response to the disease and holds true under other active planner strategies too. To be more specific, under laissez-faire, i.e., no intervention, the negative feedback mechanism engendered by the endogenous response alone

[9]The $k = 7$ strategy with low IFR is an exception. Under the baseline $VSL^{USD} = 3.81M\$$ and with lower IFR the planner narrowly prefers the 712 deaths per million and 0.17 output loss, to the 100 deaths per million and 0.22output loss, which would have made it closer to the other $7 - 7$ points.

curbs the spread of the disease; as shown in Figure 4d, $\mathcal{R}_e$ drops to below 1 in a month and subsequently converges to 1. After 18 months, only 30% of the population are infected and the ICU limit is almost never breached. Without such endogenous response, disease growth would be so rapid that even after a considerable amount of the population is infected and the susceptible pool is greatly depleted (such that $\mathcal{R}_e = 1$), it takes a while for the disease to slow down, with a considerable death toll.

At the other extreme, under full lockdown, it is not possible to eliminate the disease completely. A seed of the disease is always present in the population, or, alternatively, is imported from the outside.

These findings give perspective on the role of policy. The main aim of policy is not to "flatten the curve" or prevent an overshoot. These aims are achieved by the endogenous individual response. Policy cannot eliminate the disease or avoid its economic costs. Using lockdowns, policy is truly needed in order to "buy time." This is the time needed for individuals to adapt to the disease and for governments and for the pharmaceutical industry to develop vaccines and treatments. The question, then, is how best to do so. We show that cyclical lockdown strategies are useful in this context, as they enable the planner to smooth out the costs over a longer period of time. Doing so they reduce the total social welfare loss in PDV terms. We have analyzed the dynamics of these policies in detail, including its two modes of containment and the fact that these strategies keep $\mathcal{R}_e$ close to 1. Note that our simulations incorporate vaccine arrival time as discussed in sub-section 2.5 above and in Appendix B. Iverson, Karp, and Peri (2021) analyze and emphasize the importance of expected arrival time in this context.

6 The Cyclical Strategies vs Actual Experience

The cyclical strategies can be compared to actual real world experience. We do so by simulating optimal plans under the cyclical strategies and comparing them to a policy path based on the experience of the states of New York and Florida. The choice of these two states is motivated by the fact that both experienced high levels of the epidemic but very different dynamics.

6.1 Data and Methodology

We use state-level data on daily deaths, daily employment, lockdown measures, and the derived transmission rate, from the same sources spelled out in Appendix C for the national-level data. N_{SS} is taken to be state-level employment on March 1, 2020.

We employ the same methodology for the simulation as described above, after re-estimating the transmission equation and the endogenous response equation for each state. The equations specifications were adapted to cater for the state-specific data. For the transmission equation we used $\alpha = 1$ for both states and a different specification for β_Λ in the Florida equation. The endogenous

response equation had no time decay term, as none is apparent in the data. See the specifications delineated in the table. The estimates are reported in Table 6.

Table 6

The fit of the equations is good for the most part; the estimated κ indicates a lower endogenous response relative to the U.S. as a whole but close to the post-fatigue value in the U.S. The implication is that in both Florida and New York, employment was controlled more by the policy response and less by the endogenous response.

In New York the estimated β_t captures well the rapid drop of the reproduction parameter $\mathcal{R}_0$ from its initial value due to strict lockdown, as well as the subsequent gradual rise to values well above $\mathcal{R}_t = 1$. In Florida, the range of values for β_t, in estimation as in the data, is much narrower; for most of the time the reproduction parameter is above 1.

6.2 Results

We report the results as we did in Table 4 and Figure 5 above for the whole U.S. economy. We compare the results to actual data.[10]

Figure 6 and Table 7

Both Table 7 and Figure 6 refer to the data sample period used for the estimation reported in Table 6. The first panel of the figure looks at the data together with the cyclical strategies, while the second looks only at the latter set.

There is a substantial difference between the two states and we analyze each in turn.

New York State. As seen in Figure 6, the actual data point for NYS is very far from all the cyclical strategy points. In comparison to the cyclical strategies, the actual data exhibit a far higher death toll and just a slightly lower GDP loss. In the data the death toll is $2,346$ dead per million and the GDP loss is 0.15. The cyclical strategies entail a far lower death toll, between 7 and 29 per million, and a GDP loss of between 0.16 and 0.21, the former number being just a little above above the data number.

Looking within the cyclical set, both the second panel of Figure 6 and Table 7 show that there is variation, with the strategies using $k = 3$ and $k = 4$ being different from those using $k = 5, 6, 7, 8$. This panel depicts linear policy possibilities frontier schedules. Table 7 shows that the values of welfare losses vary across these strategies within a narrow range. The policy differences across the cyclical strategies are manifested in T_1, which values are much higher in the $k = 5, 6, 7, 8$ group, so GDP losses and welfare losses are higher. We can call the

[10] As explained in Table 4 above, GDP loss is given by

$$V_Y = \int_0^{730} e^{-rt} \left(\frac{Y^{SS}}{N^{SS}} (N^{SS} - N(t)) \right) dt$$

former group *exogenous* containment strategies, and the latter group *endogenous* containment strategies, using the terms delineated above. Only the *exogenous* containment strategies bring the average effective reproduction parameter, $\mathcal{R}_a$, to values close to unity. The *endogenous* containment strategies per se are unable to do so and do not contain the epidemic, hence the planner resorts to a very lengthy initial lockdown period (see Table 7). The reasons for this inability to contain the epidemic are two: the implied $\mathcal{R}_W$, derived from the estimated β_W, is relatively high and the estimated endogenous response parameter, κ, is relatively low.

It is clear that actual policy underperformed and achieved only weak containment. In particular, note that the use of moderately stringent cyclical tools implies a dramatic reduction in the death toll and only a slight increase in output costs relative to actual experience. Timing is key here – the optimal use of the cyclical strategies here involves an immediate initial lockdown, which proves to be critical in curbing the disease during its exponential growth phase. Compared to the optimal policy, waiting with the initial lockdown resulted in death tolls that are higher by a factor of at least 81. It thus appears that lockdown in New York State started very late and that a significant outbreak was facilitated.

Florida. This state had a death toll of $1,230$ dead per million and a GDP decline of 0.08; the cyclical strategies entail once more a far lower death toll, between 11 and 18 per million, but a bigger loss of GDP, around $0.14 - 0.17$. The cyclical strategies are able to bring the average effective reproduction parameter $\mathcal{R}_a$ to values close to unity and so to contain the epidemic. Only the $k = 3$ strategy is based on *exogenous* containment, with $\mathcal{R}_a < 1$, with all other cyclical strategies $k = 4, 5, 6, 7, 8$ based on *endogenous* containment. Initial lockdown duration, T_1, is a month and half with $k = 3$, 3-4 months for $k = 4, 5$, and longer durations for higher k values, with higher GDP losses and welfare losses.

Actual policy in Florida seems to have preferred a lower GDP decline and a much higher death toll. Using the current set-up this can be viewed from two perspectives:

(i) Absent cyclical tools, actual policy outcomes are compatible with a strategy based mostly on *endogenous* containment, such as to lock and then release until a vaccine is found, without a cyclical phase. For example, a simulation of locking for 56 days (8 weeks) and then releasing yields a GDP loss of 0.076 and a death toll of $1,306$ dead per million, very close to the data.

(ii) When cyclical tools are available, and when VSL is at $2.15M\$$, then an optimal cyclical strategy can lead to the data outcome. In panel c of Table 7 we show that a planner using $k = 10$ (which locks only on weekends) will optimally choose $T_0 = 49, T_1 = 63, T_2 = 421$, i.e., delay the initial lockdown for 7 weeks thereby letting the disease erupt, lock for two weeks, and then lock only on weekends ($k = 10$). Such a strategy yields a GDP loss of 0.079 and a death toll of $1,294$ dead per million, similar to the actual data. Note that this value of statistical life, $2.15M\$$, is 56% of our baseline value ($3.81M\$$) and is $\$152,000$ in annual terms. Such a low value, though still within the range cited by Hall, Jones, and Klenow (2020) of $\$100,000$ to $\$400,000$ per year, may have

been underlying the policy actually used in Florida.

7 Conclusions

Looking forward, the COVID19 pandemic is unlikely to be the last one. There are dozens of coronaviruses (according to CDC data, seven of which can infect humans); new influenza strains can be as deadly as the ones that have killed millions in the pandemics of the twentieth century; and Zoonotic infections (like Ebola, SARS, or zoonotic influenza) have increased significantly over time (see Jones et al. (2008) and Salyer et al. (2017)). These diseases pose an increasing and critical threat to global health security, with ever growing connectivity and mobility of people, animals, and goods. The June 2021 report of a high level G20 panel[11]states that "We are in an age of pandemics.... There is every likelihood that the next pandemic will come within a decade — arising from a new influenza strain, another coronavirus, or one of several other dangerous pathogens. Its impact on human health and the global economy could be even more profound than that of COVID-19." Meganck and Baric (2021), May (2021), and references therein, provide detailed elaboration of the key forecasted threats.

Our paper has studied the optimal timing patterns of a new, cyclical policy strategy, consisting of alternating days of opening and lockdown. Given significant trade-offs between health outcomes (deaths, breaches of ICU capacity) and economic outcomes (loss of output and employment), the analysis has shown that epidemic management policy based on such time restrictions may lead to significant improvement in terms of social welfare. The comparison was made relative to four hypothetical benchmark policies, as well as to the experience of New York State and Florida.

The analysis, which is relevant for any future epidemic, laid down the principles for time restrictions policy, as well as a framework for comparative policy analysis. Exploring this policy seems a promising avenue for future research in the context of managing epidemics. The analysis clearly shows that such time-based strategies allow for a nuanced response to observed epidemic dynamics, without resorting to singling out a particular population group. It is important to note that the afore-mentioned advantages of the cyclical strategies over prevalent policies are likely to be a lower bound of their full benefits. First, in our model the planner is deliberately constrained in the way cyclical tools are applied; for example, the planner is not permitted to mix within the set of strategies, or apply them in a staggered way. Giving the planner additional degrees of freedom, as we do for the benchmark thresholds strategies, should increase the advantages of the novel instruments over prevalent policies. Second, and not less significant, our model does not allow us to quantify the additional benefits of cyclical tools, such as the predictability of production that they entail,

[11]See the report of the High Level Independent Panel on Financing the Global Commons for Pandemic Preparedness and Response at https://pandemic-financing.org/report/foreword/

as well as their potential to alleviate part of the negative impact of prolonged isolation on mental well-being. These issues require a more elaborate analysis and are left for future research.

It should be noted that we have abstracted from heterogeneity across individuals and from modelling the coordination of work and leisure decisions. We have also abstracted from policy such as testing or contact tracing. Such issues have been addressed in the COVID19 context, albeit in different modelling frameworks, by a number of recent papers. Thus, Berger, Herkenhoff, Huang and Mongey (2022) examine how testing and targeted quarantine will work in an efficient reopening, whereby output increases while deaths are reduced. They use virological and serological testing, and their model features permanently asymptomatic individuals, incomplete information, and a reduced-form behavioral response. Chari, Kirplani, and Phelan (2021) examine how targeting of lockdown policies in a world with heterogeneity achieves better outcomes relative to indiscriminate lockdowns. Glover, Heathcote, Krueger, and Ríos-Rull (2020) analyze old-age issues and redistribution policy. Fuchs-Schündeln, Krueger, Kurmann, Lalé, Ludwig, and Popova (2021) look at the heterogeneous impact of school closures on children during COVID19. Extensions of the analysis along these lines are also left for future research.

References

[1] Abel, Andrew B. and Stavros Panageas, 2021. "Social Distancing, Vaccination and the Paradoxical Optimality of an Endemic Equilibrium," NBER Working Paper No. 27742.

[2] Abell, Martha L. and James P. Braselton, 2016. **Differential Equations with Mathematica**, 4th edition, Academic Press.

[3] Acemoglu, Daron, Victor Chernozhukov, Ivan Werning, and Michael D. Whinston, 2021. "Optimal targeted lockdowns in a multigroup SIR model." **American Economic Review: Insights** 3, 4, 487-502.

[4] Alon, Uri, Ron Milo, and Eran Yashiv, 2020. "10-4: How to Reopen the Economy by Exploiting the Coronavirus's Weak Spot," **The New York Times,** May 11**.**

[5] Alon, Uri and Eran Yashiv, 2020. "Exploiting a coronavirus weak-spot for an exit strategy," **VoxEU.org,** 27 April.

[6] Alvarez, Fernando, David Argente, and Francesco Lippi, 2021. "A Simple Planning Problem for COVID-19 Lockdown," **American Economic Review: Insights** 3, 3, 367–382.

[7] Atkeson, Andrew, 2021a. "COVID's Lessons for Future Modelling of Pandemics," **NBER Reporter**, March.

[8] Atkeson, Andrew, 2021b. "Behavior and the Dynamics of Epidemics," **Brookings Papers on Economic Activity**, March.

[9] Atkeson, Andrew, 2022. "Behavior and the Dynamics of Epidemics: An Update for Delta and Omicron" **Brookings Papers on Economic Activity**, forthcoming.

[10] Atkeson, Andrew G., Karen Kopecky, and Tao Zha, 2021. "Behavior and the Transmission of COVID-19," **AER Papers and Proceedings**111,356-60.

[11] Avery, Christopher, William Bossert, Adam Clark, Glenn Ellison, and Sara Fisher Ellison, 2020. "An Economist's Guide to Epidemiology Models of Infectious Disease" **Journal of Economic Perspectives** 34, 4, 79–104

[12] Baqaee, David, Emmanuel Farhi, Michael Mina, and James H. Stock, 2020. "Policies for a Second Wave," **Brookings Papers on Economic Activity**, **Special edition 2020: COVID-19 and the economy.**

[13] Bar-On, Yinon, Tanya Baron, Ofer Cornfeld, Ron Milo and Eran Yashiv, 2021. "Epidemiological Dynamics in the Economic Analysis of Pandemic,**"** working paper.

[14] Bar-On, Yinon, Ron Sender, Avi Flamholz, Rob Phillips, and Ron Milo, 2020. "A Quantitative Compendium of COVID-19 Epidemiology," arXiv:2006.01283; available at https://arxiv.org/abs/2006.01283

[15] Berger, David, Kyle Herkenhoff, Chengdai Huang, and Simon Mongey, 2022. "Testing and Reopening in an SEIR Model," **Review of Economic Dynamics** 43, 1–21.

[16] Blau, Francine D., Josefine Koebe, and Pamela A. Meyerhofer, 2021. "Who are the essential and frontline workers?" **Business Economics** 56, 3, 168-178.

[17] Brodeur, Abel, David Gray, Anik Islam, and Suraiya Bhuiyan, 2021. "A Literature Review of the Economics of COVID-19," **Journal of Economic Surveys** 1– 38.

[18] Brotherhood, Luiz, Philipp Kircher, Cezar Santos, and Michele Tertilt, 2021. "An Economic Model of the Covid-19 Pandemic with Young and Old Agents: Behavior, Testing and Policies," working paper.

[19] Brotherhood, Luiz and Vahagn Jerbashian, 2020. "Firm Behavior During an Epidemic," at https://sites.google.com/site/luizbrotherhood/research,

[20] Champredon, David, Jonathan Dushoff, and David J.D. Earn, 2018. "Equivalence of the Erlang-distributed SEIR Epidemic Model and the Renewal Equation," **SIAM Joural of Applied Math** 78, 6, 3258–3278.

[21] Chari, V.V., Rishabh Kirpalani, and Christopher Phelan, 2021. "The Hammer and the Scalpel: On the Economics of Indiscriminate versus Targeted Isolation Policies during Pandemics," **Review of Economic Dynamics** 42, 1–14.

[22] Chetty, R., Friedman, J. N., Hendren, N., & Stepner, M., 2020. "The Economic Impacts of COVID-19: Evidence from a New Public Database Built Using Private Sector Data, NBER Working paper 27431.

[23] Chetty, Raj, Adam Guren, Day Manoli, and Andrea Weber, 2013. "Does Indivisible Labor Explain the Difference between Micro and Macro Elasticities? A Meta-Analysis of Extensive Margin Elasticities." **NBER Macroeconomics Annual 2012**, Volume 27: 1-56.

[24] Dingel, Jonathan I. and Brent Neiman, 2020. "How Many Jobs Can be Done at Home?" **Journal of Public Economics** 189, 104235.

[25] Doelger, Julia, Arup K. Chakraborty, and Mehran Kardar, 2022. "A Simple Model for How the Risk of Pandemics from Different Virus Families Depends on Viral and Human Traits," **Mathematical Biosciences** 343,108732.

[26] Droste, Michael, and James H. Stock, 2021. "Adapting to the COVID-19 Pandemic, " **AEA Papers and Proceedings** 111, 351-55.

[27] Eichenbaum, Martin S., Sergio Rebelo, and Mathias Trabandt , 2021. "The macroeconomics of epidemics" **The Review of Financial Studies** 34, 11, 5149-5187.

[28] Farboodi, Maryam, Gregor Jarosch, and Robert Shimer, 2021. "Internal and External Effects of Social Distancing in a Pandemic," **Journal of Economic Theory** 196: 105293.

[29] Fenichel, Eli P., 2013. "Economic Considerations for Social Distancing and Behavioral Based Policies During an Epidemic" **Journal of Health Economics** 32, 440– 451.

[30] Fenichel, Eli P. , Carlos Castillo-Chavez, M. G. Ceddia, Gerardo Chowell, Paula A. Gonzalez Parra, Graham J. Hickling, Garth Holloway, Richard Horan, Benjamin Morin, Charles Perrings, Michael Springborn, Leticia Velazquez, Cristina Villalobos, 2011. "Adaptive Human Behavior in Epidemiological Models" **Proceedings of the National Academy of Sciences** 108, 15, 6306-6311.

[31] Fernandez-Villaverde, Jesus and Chales I. Jones, 2020. "Estimating and Simulating a SIRD Model of COVID-19 for Many Countries, States, and Cities," NBER Working Paper No. 27128.

[32] Fuchs-Schündeln, Nicola, Dirk Krueger, André Kurmann, Etienne Lalé, Alexander Ludwig, and Irina Popova, 2021. "The Fiscal and Welfare Effects of Policy Responses to the Covid-19 School Closures," NBER Working Paper No. 29398

[33] Garibaldi, Pietro, Espen R. Moen, and Christopher A. Pissarides, 2020. "Modelling Contacts and Transitions in the SIR Epidemics Model," **Covid Economics** 5, 16 April.

[34] Geoffard, Pierre Yves and Tomas Philipson, 1996. "Rational Epidemics and Their Public Control," **International Economic Review** 37, 3, 603-624.

[35] Glover, Andrew, Jonathan Heathcote, Dirk Krueger, Jose-Vıctor Rıos-Rull, 2020. "Health versus Wealth: On the Distributional Effects of Controlling a Pandemic," working paper.

[36] Greenstone, Michael and Vishan Nigam, 2020. "Does Social Distancing Matter?" BFI working paper no. 2020-26

[37] Greenwood, Jeremy, Philipp Kircher, Cezar Santos, and Michele Tertilt, 2019. "An Equilibrium Model of the African HIV/AIDS Epidemic" **Econometrica** 87, 4, 1081-1113.

[38] Gregory, Victoria, Guido Menzio, and David G. Wiczer, 2020. "Pandemic recession: L or V-shaped?" NBER Working Paper 27105.

[39] Hale, Thomas , Sam Webster, Anna Petherick, Toby Phillips, and Beatriz Kira, 2020. **Oxford COVID-19 Government Response Tracker.** Blavatnik School of Government.

[40] Hall, Robert E, Charles I. Jones, and Peter J. Klenow, 2020. "Trading Off Consumption and COVID-19 Deaths," **Minneapolis Fed Quarterly Review** 42, 1, 2-14.

[41] Halevy, Yoram, 2005. "Diminishing Impatience: Disentangling Time Preference from Uncertain Lifetime," working paper.

[42] Hatchett, Richard J., Carter E. Mecher, and Marc Lipsitch, 2007. "Public Health Interventions and Epidemic Intensity During the 1918 Influenza Pandemic." **Proceedings of the National Academy of Sciences** 104, 18, 7582-7587.

[43] He, X., E.H.Y. Lau, P. Wu, et al., 2020. "Temporal Dynamics in Viral Shedding and Transmissibility of COVID-19." **Nature Medicine** 26, 672–675.

[44] Huang, Chaolin, Yeming Wang, Xingwang Li, Lili Ren, Jianping Zhao, Yi Hu, et al., 2020. "Clinical Features of Patients Infected with 2019 Novel Coronavirus in Wuhan, China," **Lancet** 395: 497–506.

[45] IHME COVID-19 Forecasting Team, Reiner, R.C., Barber, R.M. et al., 2021. "Modeling COVID-19 Scenarios for the United States." **Nature Medicine** 27, 94–105.

[46] IMF, 2022. **Global Economic Outlook**, July, retrieved at https://www.imf.org/en/Publications/WEO/Issues/2022/07/26/world-economic-outlook-update-july-2022.

[47] Imperial College COVID-19 Response Team, 2020. "Report 13: Estimating the number of infections and the impact of non-pharmaceutical interventions on COVID-19 in 11 European countries," https://dsprdpub.cc.ic.ac.uk:8443/bitstream/10044/1/77731/10/2020-03-30-COVID19-Report-13.pdf

[48] Iverson, Terrence, Larry Karp, and Alessandro Peri, 2021. "Optimal Social Distancing and the Economics of Uncertain Vaccine Arrival," working paper.

[49] Johns Hopkins University CSSE, 2020. "2019 Novel Coronavirus COVID-19 (2019-nCoV) Data Repository," Center for Systems Science and Engineering.

[50] Jones, Callum J., Thomas Philippon, and Venky Venkateswaran, 2020. "Optimal Mitigation Policies in a Pandemic: Social Distancing and Working from Home," **The Review of Financial Studies** 34, 11, 5188–5223,

[51] Jones, Kate E., Nikkita G. Patel, Marc A. Levy, Adam Storeygard, Deborah Balk, John L. Gittleman, and Peter Daszak, 2008. "Global Trends in Emerging Infectious Diseases," **Nature** 451, 7181, 990-993.

[52] Kaplan, Greg, Ben Moll, and Gianluca Violante, 2020. "The Great Lockdown and the Big Stimulus: Tracing the Pandemic Possibility Frontier for the U.S." NBER Working Paper No. 27794

[53] Karin, Omer, Yinon Bar-On, Tomer Milo, Itay Katzir, Avi Mayo, Yael Korem, Avichai Tendler, Boaz Dudovich, Eran Yashiv, Amos J Zehavi, Nadav Davidovitch, Ron Milo and Uri Alon, 2020. "Adaptive Cyclic Exit Strategies from Lockdown to Suppress COVID-19 and Allow Economic Activity", MedRxiv, https://www.medrxiv.org/content/10.1101/2020.04.04.20053579v4.full.pdf

[54] Kermack, William O., and Anderson G. McKendrick, 1927. "A Contribution to the Mathematical Theory of Epidemics," **Proceedings of the Royal Society London**. Ser. A., 115, 700–721.

[55] Kong, D., Zheng, Y., Wu, H., Pan, H., Wagner, A.L., Zheng, Y., Gong, X., Zhu, Y., Jin, B., Xiao, W. and Mao, S., 2020. Pre-symptomatic transmission of novel coronavirus in community settings. **Influenza and other respiratory viruses**, 14, 6, 610-614

[56] Kotz, Samuel and Saralees Nadarajah, 2000. **Extreme Value Distributions: Theory and Applications**. World Scientific, Singapore.

[57] Krueger, Dirk, Harald Uhlig, and Taojun Xie, 2020. "Macroeconomic Dynamics and Reallocation in an Epidemic," NBER Working Paper No. 27047

[58] Lawson, Charles L. and Richard J. Hanson, 1995. **Solving Least Squares Problems**. Classics in Applied Mathematics, SIAM, Philadelphia.

[59] Li, Guanlin, Shivam Shashwat, Michael E. Hochberg, Yorai Wardi, and Joshua S. Weitz, 2021. "Disease-dependent interaction policies to support health and economic outcomes during the COVID- 19 epidemic," **iScience** 24, 102710.

[60] Li, Ruiyun , Sen Pei, Bin Chen, Yimeng Song, Tao Zhang, Wan Yang, and Jeffrey Shaman, 2020. "Substantial Undocumented Infection Facilitates the Rapid Dissemination of Novel Coronavirus (SARS-CoV-2)," **Science** 368, 6490, 489-493.

[61] Ma, Shujuan, Jiayue Zhang, Minyan Zeng, Qingping Yun, Wei Guo, Yixiang Zheng, Shi Zhao, Maggie H. Wang, and Zuyao Yang, 2021. "Epidemiological parameters of coronavirus disease 2019: a pooled analysis of publicly reported individual data of 1155 cases from seven countries." Medrxiv, https://www.medrxiv.org/content/10.1101/2020.03.21.20040329v1

[62] May, Milke, 2021. "Tomorrow's Biggest Microbial Threats," **Nature Medicine** 27, 358–359.

[63] Meganck, Rita M. and Ralph S. Baric, 2021. "Developing Therapeutic Approaches for Twenty-first-century Emerging Infectious Viral Diseases." **Nature Medicine** 27, 401–410.

[64] Meyerowitz-Katz, Gideon and Lea Merone, 2020. "A Systematic Review and Meta-Analysis of Published Eesearch Data on COVID-19 Infection Fatality Rates, **International Journal of Infectious Diseases**, 101, 138-148,

[65] Mills, Christina E., James M. Robins, and Marc Lipsitch, 2004. "Transmissibility of 1918 Pandemic Influenza, " **Nature** 432, 904-906.

[66] Murphy, Kevin M., and Robert H. Topel, 2006. "The Value of Health and Longevity," **Journal of Political Economy** 114, 5, 871-904.

[67] Nature Medicine, 2021. "Preparing for the Next Pandemic," **Nature Medicine** 27, 357.

[68] Pagel, Christina, 2022. ""Back to Normal" is Not Enough," **Science** 375, 6585, 1069.

[69] Philipson, Tomas, 2000. "Economic Epidemiology and Infectious Diseases," Chapter 33 in Anthony J. Culyer and Joseph P. Newhouse (eds) **Handbook of Health Economics** Volume 1, Part B, 1761-1799, Elsevier.

[70] Ren, Xiang, Yu Li, Xiaokun Yang, Zhili Li, Jinzhao Cui, Aiqin Zhu, Hongting Zhao et al., 2021. "Evidence for pre-symptomatic transmission of coronavirus disease 2019 (COVID-19) in China." **Influenza and other respiratory viruses** 15, 1, 19-26.

[71] Richardson Safiya, Jamie S. Hirsch, Mangala Narasimhan, et al., 2020. "Presenting Characteristics, Comorbidities, and Outcomes Among 5700 Patients Hospitalized With COVID-19 in the New York City Area." **JAMA** 323(20):2052–2059.

[72] Salje, Henrik, Cecile Tran Kiem, Noemie Lefrancq, Noemie Courtejoie, Paolo Bosetti, Juliette Paireau, et al., 2020. "Estimating the Burden of SARS-CoV-2 in France," **Science** 369, 208–211.

[73] Salyer, Stephanie J., Rachel Silver, Kerri Simone, and Casey Barton Behravesh, 2017. "Prioritizing Zoonoses for Global Health Capacity Building, Themes from One Health Zoonotic Disease Workshops in 7 Countries, 2014–2016." **Emerging Infectious Diseases** 23, Suppl 1: S55.

[74] Tian, Huaiyu Yonghong Liu, Yidan Li, Chieh-Hsi Wu, Bin Chen, Moritz U. G. Kraemer, Bingying Li, et al., 2020. "An Investigation of Transmission Control Measures During the First 50 Days of the COVID-19 Epidemic in China," **Science** 368(6491), 638-642. https://doi.org/10.1126/science.abb6105

[75] Tindale, Lauren C., Jessica E. Stockdale, Michelle Coombe, Emma S. Garlock, Wing Yin Venus Lau, Manu Saraswat, Louxin Zhang, Dongxuan Chen, Jacco Wallinga, and Caroline Colijn, 2021. "Evidence for transmission of COVID-19 prior to symptom onset." **Elife** 9, e57149.

[76] Verelst, Frederik, Willem Lander, and Philippe Beutels, 2016. "Behavioural change models for infectious disease transmission: a systematic review (2010– 2015)," **Journal of the Royal Society, Interface** 13:2016082

[77] Wallinga,Jacco, Michiel van Boven, and Marc Lipsitch, 2010. " Optimizing Infectious Disease Interventions During an Emerging Epidemic" **Proceedings of the National Academy of Sciences** 107, 2, 923–928.

[78] Wearing, Helen J., Pejman Rohani, and Matt J. Keeling, 2005. " Appropriate Models for the Management of Infectious Diseases," **PLoS Medicine** 2, 7, 621-627**.**

[79] Yashiv, Eran, 2020. "How to Reopen Society More Quickly," **Financial Times**, April 21.

8 Tables and Figures

Figure 1: The Model

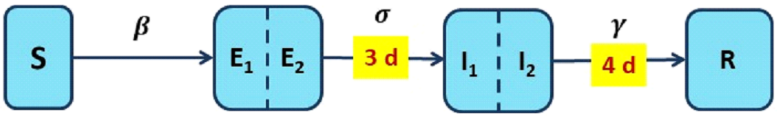

a. The SEIR-Erlang block

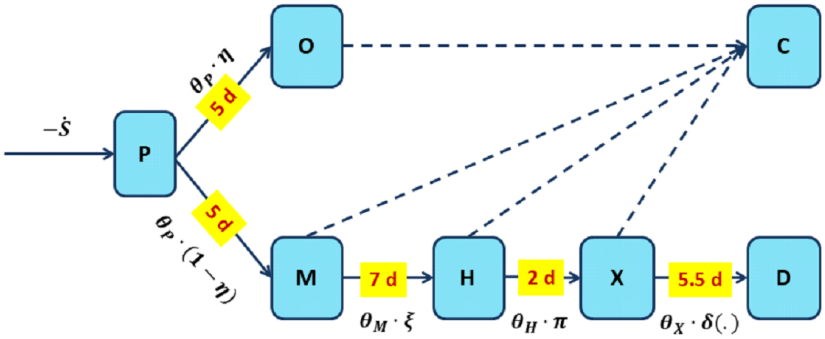

b. The Clinical block

Table 1: Menu of the Cyclical Strategies

					week 1							week 2						
k	Strategy	Workdays locked			M	T	W	T	F	S	S	M	T	W	T	F	S	S
		week 1	week 2	in total														
0	lockdown only	5	5	10														
3	3-11	2	5	7														
4	4-10	1	5	6														
5	week on, week off	0	5	5														
6	3-day week	2	2	4														
7	7-7	1	2	3														
8	long weekend	1	1	2														
14	no intervention	0	0	0														

Locked Open

Note:
k is the number of open (non-lockdown) days every 14 days.

Figure 2: Alternative Distributions of Waiting Time till Vaccine Arrival

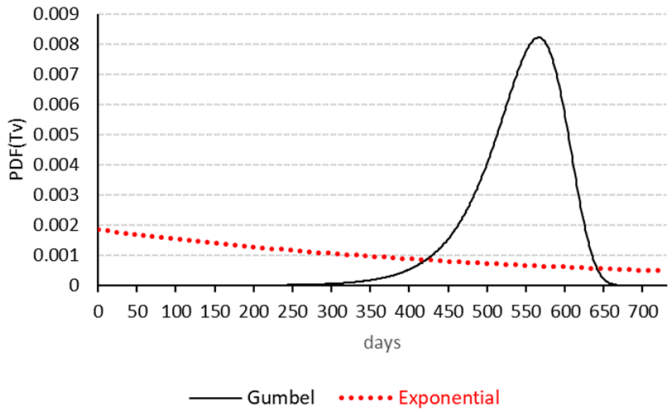

Note: The parameter of the exponential distribution is set to 1/540, and the location and scale of Gumbel distribution are set to 565.83 and 44.74, respectively.

Table 2: Calibration

Parameter	Interpretation	Range	value
a. The Infection Transmission Block (SEIR)			
σ	latent period duration	$3-5$ days	$1/3$
γ	infectious period duration	$4-5$ days	$1/4$
b. The Clinical Block			
θ_P	incubation period	$5-6$ days	$1/5$
θ_M	days from symptoms till hospitalization	7 days	$1/7$
θ_H	days in hospital till ICU	2 days	$1/2$
θ_X	days in ICU before death	5.5 days	$1/5.5$
η	Prob. to be asymptomatic	$20\%-50\%$	0.5
ξ	Prob.of hospitalization when symptomatic	$\frac{\#Hospitalized}{\#Infected} = [2\%-4\%]$	$\frac{0.04}{1-0.5} = 0.08$
π	Prob. of ICU admission	$10\%-40\%$	0.4
IFR	Infection Fatality Rate (implied)		0.008

Sources:

1. Panel a: Bar-On et al (2020); He at al (2020); Li et al (2020); Tian et al (2020);

2. Panel b – Bar-On et al (2020); Huang et al (2020); Richardson et al (2020); Salje et al (2020).

Notes:

a.. Range relates to number of days, unless noted otherwise.

b. $\frac{\#Hospitalized}{\#Infected} = \frac{\#Hospitalized}{\#Symptomatic} \cdot \frac{\#Symptomatic}{\#Infected} = \xi \cdot (1-\eta) \implies \xi = \frac{\frac{\#Hospitalized}{\#Infected}}{1-\eta}$

c.. $IFR = \xi \cdot \pi \cdot \eta \cdot \delta_1$

Figure 3: Key Variables

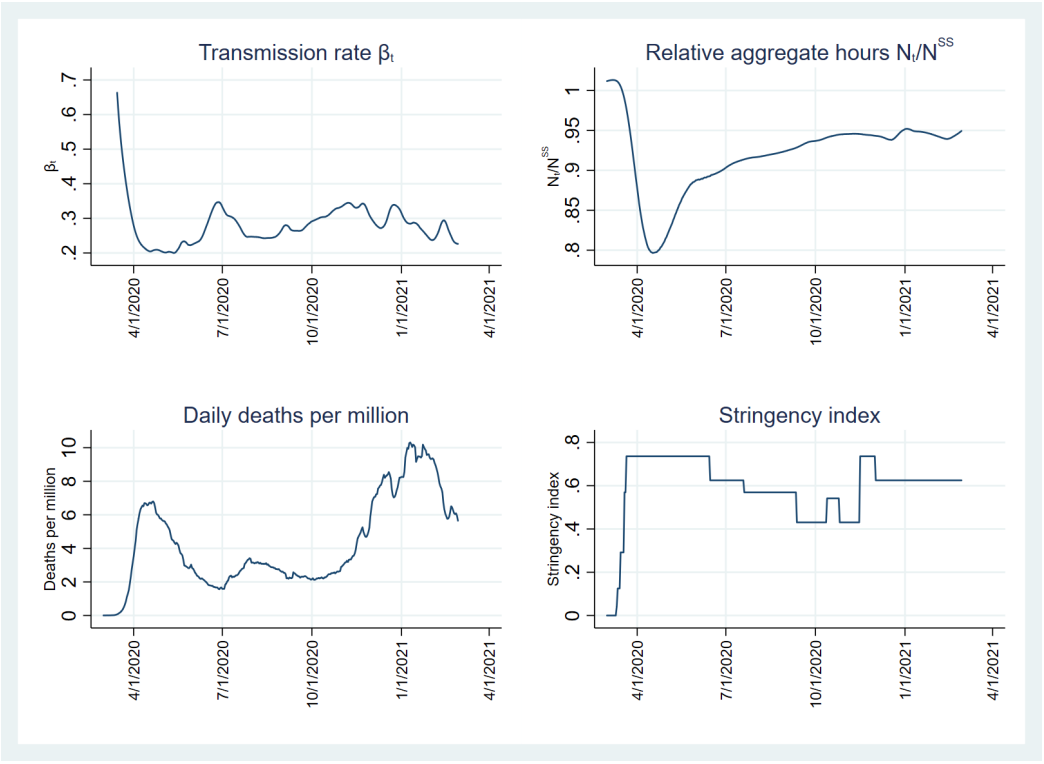

Notes:
Data sources and definitions are elaborated in Appendix C.

Table 3
Estimation Results

a. Infection Transmission

$$\beta_t = \beta_W - \beta_N \left(1 - \frac{N_t}{N^{SS}}\right)^{\alpha} + \beta_\Lambda \exp\left(-\Lambda t\right)$$

March 15, 2020-February 28, 2021

β_Λ	Λ	β_W	β_N	α
0.339^{***}	0.12^{***}	0.376^{***}	0.53^{***}	0.69
(0.05)	(0.01)	(0.05)	(0.12)	(0.31)

R^2	0.74
$RMSE$	0.0307
n	351

b. The Endogenous Response

$$\frac{N_t}{Nss} = 1 - \max(\varkappa_t L_t, \kappa_t \dot{D}_t) + \varepsilon_t$$

March 1, 2020-February 28, 2021

κ	φ_κ	$\varkappa$	$\varphi_\varkappa$	μ_f	σ_f
0.095^{***}	0.18^{***}	0.42^{***}	0.59^{***}	245^{***}	27.5^{***}
(0.0001)	(0.01)	(0.007)	(0.026)	(2.36)	(2.68)

R^2	0.99
$RMSE$	0.0139
n	365

Notes
a. Tables report point estimates with s.errors in parentheses.
b. $^{*}p < 0.10,^{**}p < 0.05,^{***}p < 0.01$

Table 4: Outcomes of the Different Policy Strategies – Baseline

		T_0	T_1	T_2	WL (utility)	WL (cons)	GDP loss	D (per 10^6)
				Non-cyclical				
(i)	No Intervention	540	540	540	68.70	0.361	0.098	2,482
(ii)	Full lockdown	0	540	540	46.75	0.291	0.287	21
(iii)	Thresholds	*n.a.*	*n.a.*	*n.a.*	38.35	0.248	0.201	425
(iv)	Optimal L ($k=0$)	8	487	487	42.24	0.268	0.256	84
				Cyclical				
(v)	$k=3$	0	14	499	34.65	0.226	0.211	43
(vi)	$k=4$	0	14	511	32.95	0.221	0.197	76
(vii)	$k=5$	0	98	534	33.30	0.218	0.201	42
$(viii)$	$k=6$	0	120	540	36.14	0.240	0.194	218
(ix)	$k=7$	0	296	540	38.68	0.252	0.224	113
(x)	$k=8$	0	366	540	39.75	0.257	0.236	75

Notes:

a. We use

$$\overline{g} = 0.32, VSL^{USD} = 3.81M\$, IFR = 0.8\%$$

b. T_0 is the start day of lockdown, T_1 start day of the cyclical strategy, and T_2 the release day; the numbers in these columns indicate day number since the start of the epidemic. The assumption is that vaccine arrival happens on day 540.

c. Welfare loss (utility) – the realized welfare loss when the vaccine actually arrives on day 540, in PDV terms, i.e., **the loss** of W, which is defined as follows:

$$WL\left(n_t, \dot{D}_t\right) \equiv \widetilde{V}\left(n_{ss}, 0\right) - \widetilde{V}_t\left(n_t, \dot{D}_t\right)$$

where $\widetilde{V}_t$ is the planner instantaneous utility and $U\left(n_{ss}, 0\right) = \widetilde{V}\left(n_{ss}, 0\right)$ is steady state utility with no deaths, and

$$\widetilde{V}\left(n_t, \dot{D}_t\right) = \ln\left(w \cdot n_t\right) - \frac{1}{5}\left(\frac{n_t}{n_{ss} \cdot \omega^x(\dot{D}_t, t)}\right)^5 - \ln \omega^x(\dot{D}_t, t) - VSL^U \cdot \dot{D}_t$$

d. Welfare loss (consumption terms) – the realized welfare loss when the vaccine actually arrives on day 540, in PDV terms, in consumption terms as given by:

$$PDV\_CL\left(WL_t\right) = \int_{t=0}^{\infty} \exp\left(-rt\right) CL\left(WL_t\right) dt$$

where

$$CL\left(WL_t\right) = 1 - \frac{WL_0^{-1}\left(WL_t\right)}{n_{ss}}$$

See sub-section 2.4 for details.
d. GDP loss – loss in GDP terms computed as:

$$V_Y = \int_0^{730} e^{-rt}\left(\frac{Y_{ss}}{N_{SS}}(N_{SS} - N_t)\right)dt$$

e. Cumulative deaths D (per 10^6) – stock of death per million.

Figure 4
Six Policy Strategies

a. $k = 4, 5, 8$

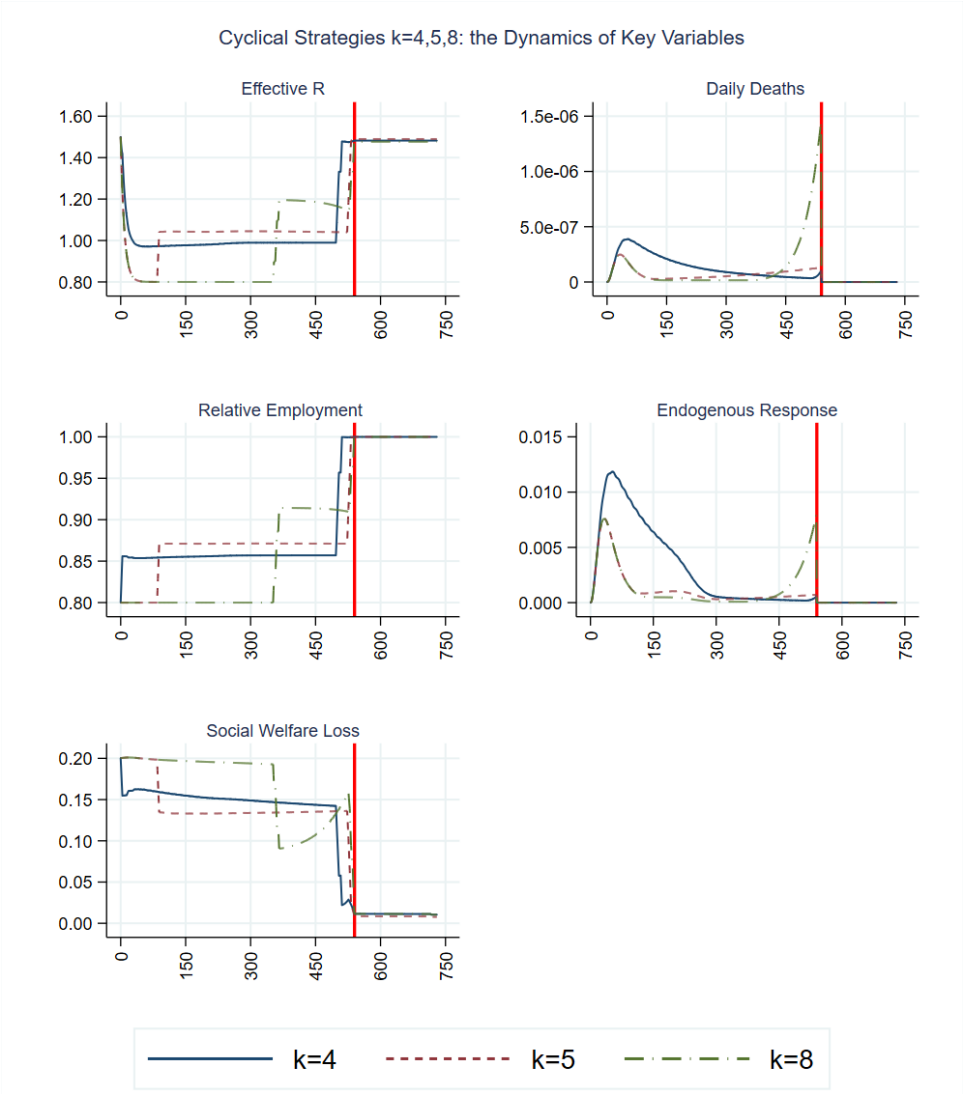

b. $k = 5$ **and benchmarks**

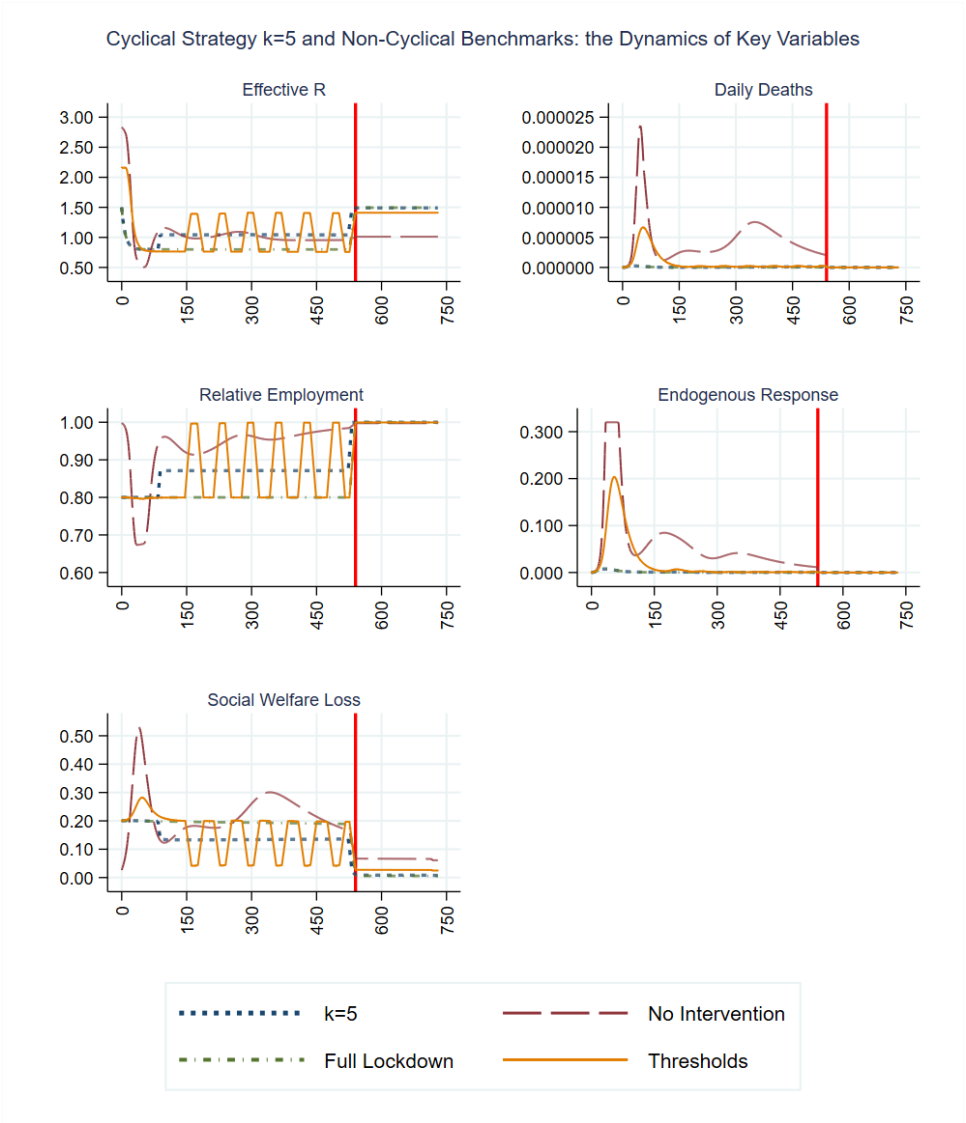

Notes:

a. The series plotted are as follows: the effective reproduction parameter $\mathcal{R}_e$, flow deaths $(\dot{D}_t)$, the employment level relative to its pre-epidemic steady state $\frac{N_t}{N_{SS}}$, the endogenous response $\kappa_t D_t$, and the flow welfare loss in consumption terms $PDV\_CL\,(WL_t)$, as computed from equations (47)-(48).

b. For all series, except for the endogenous response, we use a smoothed 14 day average.

Figure 5: The Policy Frontier

a. Cyclical and Benchmark Strategies

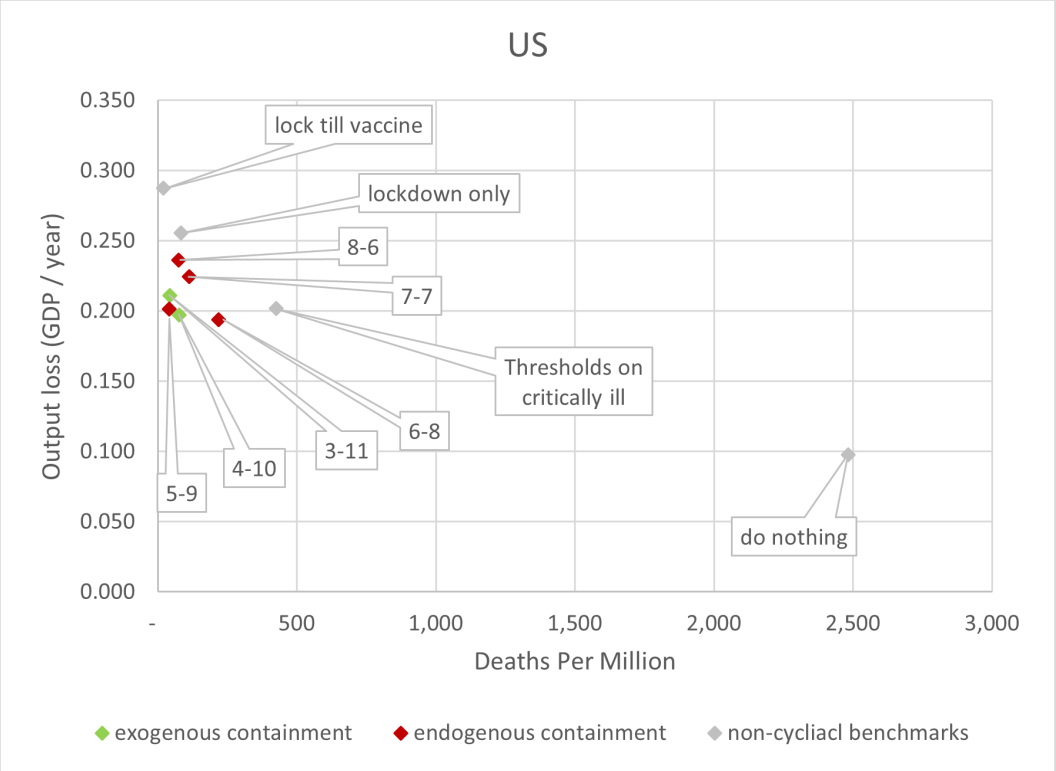

Notes:
See notes d and e to Table 4.

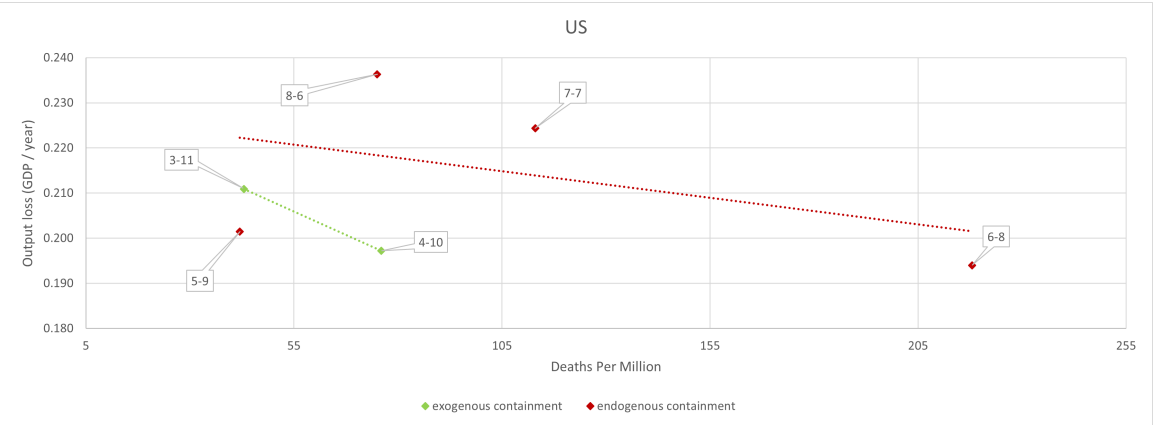

Note:
Second graph is a "zoom-in" on the first graph.

b. Alternative Values of IFR

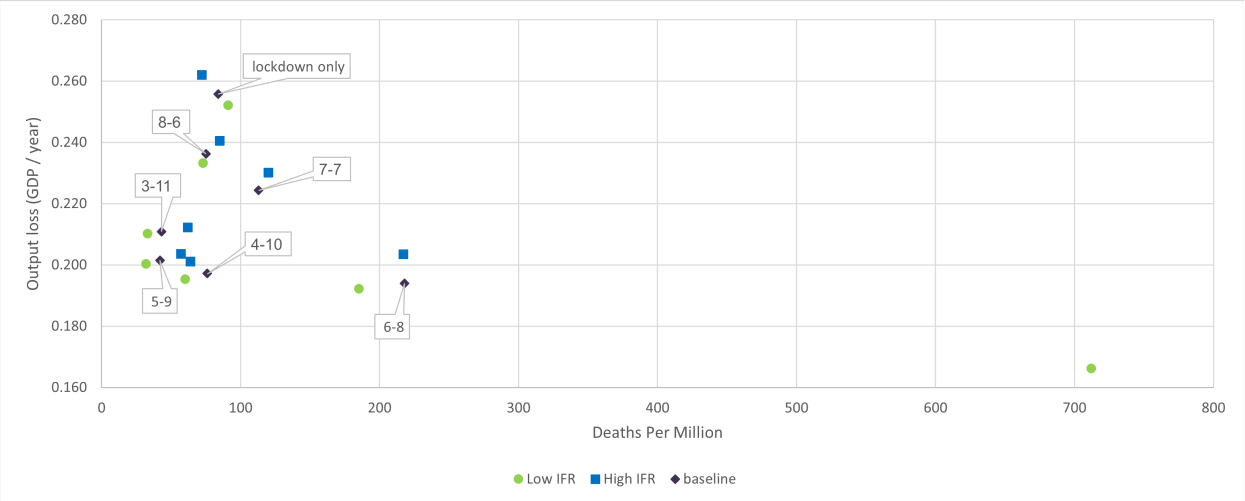

Notes:

a. Legend is

color	IFR
blue	high, 1.2%
black	baseline, 0.8%
green	low, 0.6%

b. For each IFR value we plot strategies $k = 3...8$. These are labelled only for the black points.

Table 5

Parameter Variations – IFR

value of life: $IFR = 0.6\%$						
k	$k=3$	$k=4$	$k=5$	$k=6$	$k=7$	$k=8$
T_0	0	0	0	0	18	0
T_1	14	14	98	113	35	352
T_2	498	507	530	540	540	540
WL (utility)	34.44	32.49	32.99	35.26	39.02	39.31
WL (cons)	0.224	0.217	0.215	0.235	0.262	0.254
Output loss	0.210	0.195	0.200	0.192	0.166	0.233
D (per 10^6)	33	60	32	185	712	73

value of life: $IFR = 1.2\%$						
k	$k=3$	$k=4$	$k=5$	$k=6$	$k=7$	$k=8$
T_0	0	0	0	0	0	0
T_1	14	37	99	162	317	380
T_2	501	509	540	540	540	540
WL (utility)	35.05	33.37	33.85	37.42	39.56	40.47
WL (cons)	0.230	0.221	0.223	0.247	0.257	0.261
output loss	0.212	0.201	0.204	0.204	0.230	0.240
D (per 10^6)	62	64	57	217	120	85

Notes: See Table 4.

Table 6
Estimation Results for New York State and Florida

a. New York State, March 15, 2020 to February 28, 2021.

a. Infection Transmission

$$\beta_t = \beta_W - \beta_N \left(1 - \frac{N_t}{N^{SS}}\right) + \beta_\Lambda \exp\left(-\Lambda t\right)$$

β_Λ	Λ	β_W	β_N
0.202	0.967***	0.517***	1.519***
(0.437)	(1.777)	(0.0112)	(0.0797)

R^2	0.559
$RMSE$	0.0631
n	351

b. The Endogenous Response

$$\frac{N_t}{Nss} = 1 - \max(\varkappa L_t, \kappa \dot{D}_t) + \varepsilon_t$$

κ	$\varkappa$
0.00506***	0.224***
(0.000218)	(0.00274)

R^2	0.998
$RMSE$	0.0339
n	352

Notes
a. The tables report point estimates with s.errors in parentheses.
b. $^{*}p < 0.10,^{**}\ p < 0.05,^{***}\ p < 0.01$

b. Florida, March 27, 2020 to January 31, 2021

a. Infection Transmission

$$\beta_t = \beta_W - \beta_N \left(1 - \frac{N_t}{N^{SS}}\right) + (\beta_{Max} - \beta_W) \exp(-\Lambda t)$$

Λ	β_W	β_N
0.0912	0.329^{***}	0.496^{***}
(0.174)	(0.0121)	(0.135)

$\beta_{Max} = 0.364$

R^2	0.971
$RMSE$	0.0495
n	311

b. The Endogenous Response

$$\frac{N_t}{Nss} = 1 - \max(\varkappa L_t, \kappa \dot{D}_t) + \varepsilon_t$$

κ	$\varkappa$
0.0118^{***}	0.174^{***}
(0.000754)	(0.00334)

R^2	0.999
$RMSE$	0.0326
n	324

Notes
a. Tables report point estimates with s.errors in parentheses.
b. $^{*}p < 0.10,^{**}p < 0.05,^{***}p < 0.01$

Figure 6
Policy Possibilities Frontier Plots for New York State and Florida

a. NYS, March 15, 2020 and February 28, 2021.

1. General

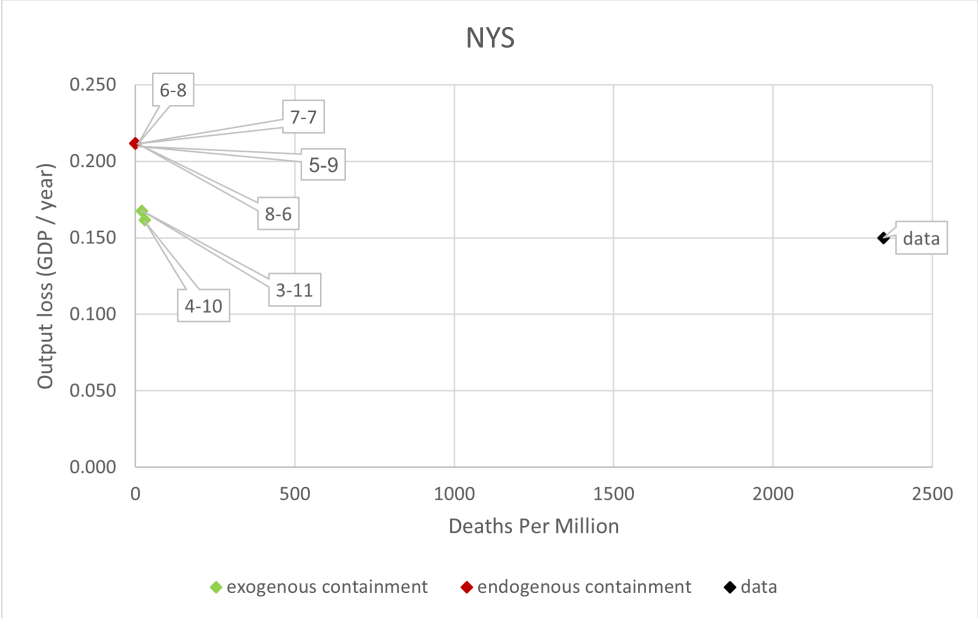

2. Zoomed in

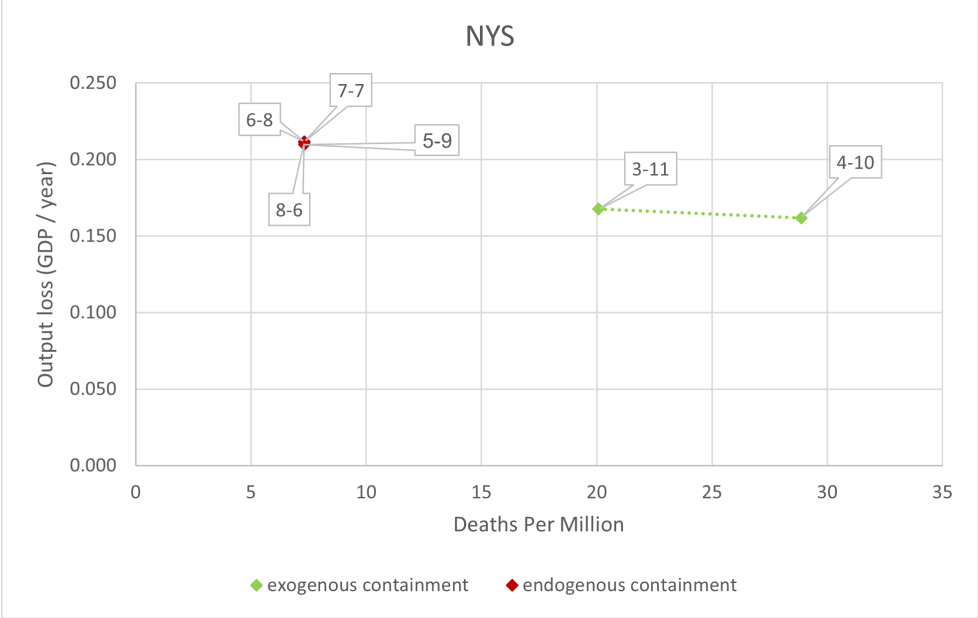

b. Florida, March 27, 2020 to January 31, 2021.

1. General

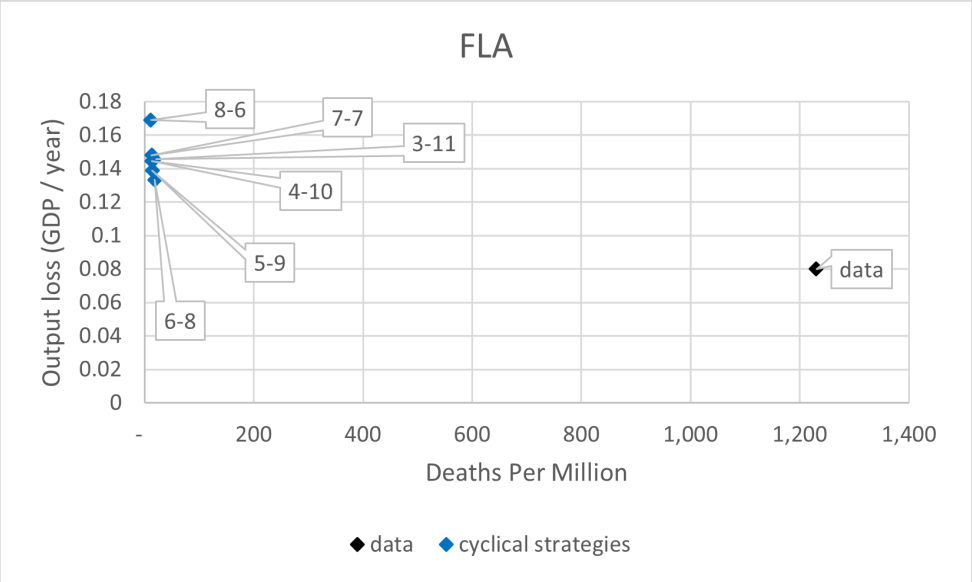

2. Zoomed in

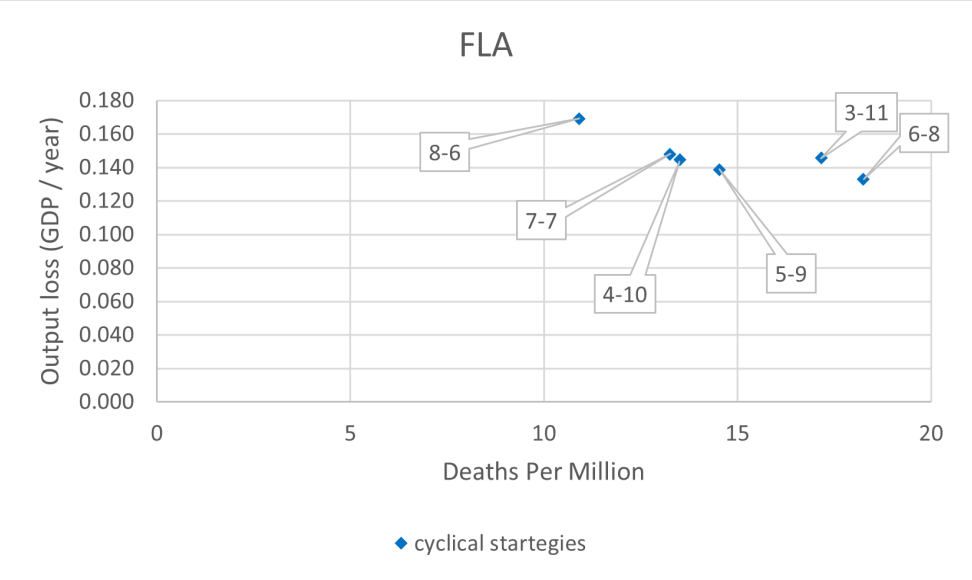

Notes:
See notes d and e of Table 4.

Table 7
State Level Outcomes
(at the end of the sample period)

a. New York State - March 15, 2020 and February 28, 2021.

		T_0	T_1	T_2	WL (utility)	WL (cons)	GDP loss	D (per 10^6)
$L_L = 0.22; VSL^{USD} = 3.81M\$; IFR = 0.8\%$								
(i)	$k = 3$	0	14	540	29.45	0.170	0.168	20
(ii)	$k = 4$	3	58	540	28.41	0.165	0.160	33
(iii)	$k = 5$	0	345	540	36.43	0.206	0.210	7
(iv)	$k = 6$	0	449	540	36.74	0.208	0.212	7
(v)	$k = 7$	0	479	540	36.74	0.208	0.212	7
(vi)	$k = 8$	0	500	540	36.74	0.208	0.212	7

b. Florida, March 27, 2020 to January 31, 2021

		T_0	T_1	T_2	WL (utility)	WL (cons)	GDP loss	D (per 10^6)
$L_L = 0.21; VSL^{USD} = 3.81M\$, IFR = 0.8\%$								
(i)	$k = 3$	0	44	449	24.55	0.148	0.146	17
(ii)	$k = 4$	0	105	473	24.30	0.146	0.144	14
(iii)	$k = 5$	0	115	506	23.38	0.141	0.139	15
(iv)	$k = 6$	0	127	540	22.52	0.137	0.133	18
(v)	$k = 7$	0	205	540	24.90	0.149	0.148	13
(vi)	$k = 8$	0	282	540	28.35	0.168	0.169	11

c. Florida, March 27, 2020 to January 31, 2021 , VSL=$2.15M\$$

		T_0	T_1	T_2	WL (utility)	WL (cons)	GDP loss	D (per 10^6)
$L_L = 0.21; VSL^{USD} = 2.15M\$, IFR = 0.8\%$								
(i)	$k = 4$	49	63	444	23.18	0.142	0.115	469
(ii)	$k = 6$	49	63	454	23.37	0.144	0.100	741
(iii)	$k = 8$	49	63	442	24.63	0.149	0.089	1039
(iv)	$k = 10$	49	63	421	25.99	0.154	0.080	1294

Notes:
1. See Section 7 of the paper.
2. See the notes to Table 4.